
Ancient TL

www.ancienttl.org · ISSN: 2693-0935

Issue 27(2) - December 2009

<https://doi.org/10.26034/la.atl.v27.i2>

This issue is published under a Creative Commons Attribution 4.0 International (CC BY):

<https://creativecommons.org/licenses/by/4.0>



© Ancient TL, 2009

The Clermont radiometric reference rocks: a convenient tool for dosimetric purposes

D. Miallier¹, G. Guérin², N. Mercier², T. Pilleyre¹ and S. Sanzelle¹

1. Laboratoire de Physique Corpusculaire (LPC), Université Blaise Pascal, CNRS/IN2P3, UMR 6533, F-63177 Aubière cedex, France

2. Institut de Recherche sur les Archéomatériaux, UMR 5060 CNRS - Université de Bordeaux, Centre de Recherche en Physique Appliquée à l'Archéologie (CRP2A), Maison de l'archéologie, 33607 Pessac cedex, France

(Received 14 October 2009; in final form 6 November 2009)

Abstract

Boreholes drilled in 8 different rocks situated in the vicinity of the Clermont TL laboratory have been used for testing and calibrating methods devoted to measurement of natural radioactivity. The present paper gives updated data for the nuclide contents and internal dose rates for those reference media. Two examples of application are presented. The first example shows dose rate calibration of a scintillator gamma probe using a threshold method. The second example shows a routine technique for TL dosimetry, based on the rocks for dose rate reference.

Introduction

Various experiments aimed at testing or calibrating techniques devoted to the measurement of natural gamma and X-ray emissions necessitate reference homogeneous media of well known radioactivity. For this purpose, the Clermont TL group (Clermont-Ferrand, France) has been using natural rocks for many years (Sanzelle et al., 1988; Miallier et al., 1988; Soumana et al., 1994). This approach has also been adopted by other luminescence dating groups (Prescott and Hutton, 1988). The use of rocks is an alternative to built blocks such as those prepared at Oxford University with doped concrete (Murray, 1982; Aitken, 1985) or those made of building bricks available in different laboratories (e.g. Gif-sur-Yvette and Bordeaux). One advantage of natural rocks is that they can easily provide homogeneous media, large enough to represent an infinite volume from the point of view of natural gamma emissions. This is particularly the case for lava flows, which, moreover, are numerous in the vicinity of Clermont-Ferrand. In contrast, the laboratory blocks have generally dimensions lower than the maximal range of the most energetic natural gamma rays. For instance, the cubic Oxford blocks (side = 50 cm) have a thickness (50 g.cm⁻²) which is only equal to around two mean free paths for the 2.61 MeV photons emitted by ²⁰⁸Tl.

Additionally, it is suspected that the Oxford blocks are affected by radon loss in proportions which might attain 10% (Aitken, Pers. com., 2009 and Bowman, 1976). Such effects have to be accounted for in certain calculations, such as, for example, evaluating the factor between the nuclide content and the derived induced radiation dose rate (Soumana, 1993; Rhodes and Schwenninger, 2007).

However, the inner radioactivity of naturally occurring rocks is not determined in the course of construction, as it can be theoretically with doped blocks; this can be a drawback for certain experiments using rocks.

Since the beginning of the 1980's, a dozen boreholes were drilled in a variety of rocks whose bare surfaces were exposed either naturally or by human action. These different sites are situated within 25 km of the laboratory. Recently, in order to reduce the distance to be travelled for experiments, two large blocks, weighing 10.5 t and 9.5 t were transported close to the laboratory (Fig.1).



Figure 1: Drilling the block of granite C347, weighing 9500 kg

Reference	SiO ₂	Al ₂ O ₃	Fe ₂ O ₃	MgO	CaO	Na ₂ O	K ₂ O	TiO ₂	P ₂ O ₅	MnO	H ₂ O		total	Nature
											(1000°C)	(110°C)		
PEP	60.0	16.2	5.6	2.85	3.19	3.36	4.63	0.84		0.08	2.1	0.11	98.96	granite
LAS	49.5	16.0	10.6	5.67	8.68	4.21	2.33	2.25		0.18	0.21	0.26	99.89	basalt
LMP	42.9	12.6	12.8	10.6	11.1	2.64	0.87	2.84		0.17	2.1	1.06	99.75	basalt
MPX	86.0	6.89	0.83	0.11	0.07	0.19	3.08	0.05		0.01	1.35	0.1	98.59	sandstone
MAZ	49.19	17.13	12.12	4.69	8.47	4.36	2.24	2.39		0.2	0	0.33	100.07	trachyandesite
GOU	54.9	18.2	7.91	2.25	5.47	5.4	3.13	1.38		0.22	0	0.03	98.9	trachyandesite
C347	73.09	15.05	1.45	0.38	0.89	3.62	4.27	0.13	0.19			0.82	99.79	granite
C341	46.95	16.67	12.15	6.16	9.59	3.71	1.65	2.44	0.57	0.19	0.17		100.28	trachybasalt

Table 1: Composition and nature of the reference rocks

On the other hand, some sites are no longer accessible at present, so that 8 reference rocks are currently available (and possibly 2 more, slightly less convenient). The boreholes are horizontal, they have a diameter of 70 mm and a length between 0.39 m and 1.5 m. The cores extracted in the course of drilling were crushed and homogenized before being distributed among several laboratories for elemental analyses, including nuclide assessment. Some of the nuclide analyses gave rise to inter-laboratory comparisons (Faïn et al., 1997). Dose rates in the different rocks were derived from the nuclide contents. Dose rate measurements were also performed in situ, in the holes, by independently calibrated means including TL dosimeters and NaI gamma probes.

This paper is aimed at giving updated data for those reference media and at presenting two examples of their use. The first one concerns the calibration of a field probe for gamma dose rate measurements. The second one is a simple and advantageous method for TL dosimetry, where the reference rocks are used as radiation-dose-sources, avoiding the use of a laboratory calibrated source.

Data concerning the reference rocks

The reference rocks include two granites, one sandstone and six lavas (Table 1). Apart from the two blocks settled close to the laboratory (C341 and C347), the rocks do not appear as free blocks, but as outcrops in geologic massive formations. Homogeneity at the metre scale around the boreholes is assumed from the geological nature of the rocks, which are not bedded, and from visual inspection. The water content is nil, or low but stable. Certain lavas are porous; however the pores are not interconnected, so that time-variation in water content is not possible. Although the holes are

horizontal, they may sometimes be wet inside, due to rain, but this cannot affect the dose rate.

The nuclide contents of the rocks were assessed by various laboratory methods, comprising: low background gamma spectrometry, ICP-MS, NAA and flame photometry (for K). ²³⁰Th was measured by means of alpha spectrometry for recent lavas since these can show a slight disequilibrium in the U-series.

The nuclide contents were also verified in situ for C341 and C347 by using a NaI gamma probe. The laboratories or persons who participated in the measurements are listed in Annex 1.

Reference	[U] ppm	[Th] ppm	²³⁰ Th/ ²³⁸ U	²²⁶ Ra/ ²³⁰ Th
PEP	6.00 ± 0.20	19.0 ± 2.0	1	1
LAS	2.14 ± 0.04	7.57 ± 0.15	1	1
LMP	1.60 ± 0.14	5.91 ± 0.09	1	1
MPX	1.38 ± 0.03	3.61 ± 0.20	1	1
MAZ	2.39 ± 0.08	8.58 ± 0.04	1.00 ± 0.01	1.07 ± 0.01
GOU	3.18 ± 0.12	11.95 ± 0.06	1.00 ± 0.01	1.11 ± 0.01
C 347	2.84 ± 0.12	4.67 ± 0.10	1	1
C 341	1.80 ± 0.05	6.42 ± 0.40	1.10 ± 0.01	1.0 ± 0.01

Table 2: Nuclide contents of the reference rocks. The ²³⁰Th/²³⁸U and ²²⁶Ra/²³⁰Th ratios are given for activities. For the older rocks, PEP, LAS, LMP, MPX, and C347, these ratios were not measured; they were inferred from the ages of the rocks (3 Ma for the youngest one, LMP). Uncertainties are quoted at the 95% level of confidence.

Reference	D_γ $\mu\text{Gy}\cdot\text{a}^{-1}$	D_{cosmic} $\mu\text{Gy}\cdot\text{a}^{-1}$	Total
PEP	2536 ± 110	140 ± 14	2676 ± 110
LAS	1082 ± 10	120 ± 20	1202 ± 22
LMP	641 ± 18	120 ± 20	761 ± 27
MPX	962 ± 13	110 ± 15	1072 ± 20
MAZ	1140 ± 12	200 ± 20	1340 ± 23
GOU	1573 ± 17	110 ± 11	1683 ± 23
C347	1421 ± 25	170 ± 18	1591 ± 29
C341	849 ± 21	170 ± 18	1019 ± 26

Table 3: Gamma and cosmic dose- rates in the reference rocks. Gamma dose rates were calculated using the data of Adamiec and Aitken (1998) revised for ^{40}K and the Th-series by Guérin and Mercier (submitted). Cosmic dose rates were derived from the data of Prescott and Hutton (1994).

The gamma dose rates in the different media were calculated on the basis of the conversion coefficients published by Adamiec and Aitken (1998), and the updated coefficients given by Guérin and Mercier (submitted) for ^{40}K and the Th-series. Allowance was made for disequilibrium where necessary. The cosmic contribution was evaluated using the data of Prescott and Hutton (1994).

Radon loss has not been specifically measured. It has been considered as negligible for all the rocks, because of their compactness and it has been indirectly verified by the good agreement between the calculated dose rates and the in situ measured dose rates. Moreover, the activity ratios $^{210}\text{Pb}/^{226}\text{Ra}$ for the rocks are not significantly differing from 1.

Application to the calibration of a portable gamma spectrometer

The Clermont reference rocks were used for calibrating a probe aimed at being a convenient tool for gamma dose rate determinations in the field. The detecting cell of the probe is made of a 1.5" x 1.5" scintillation crystal (LaBr_3). According to the manufacturer (Canberra), this material exhibits a higher detection efficiency and a higher resolution than the more classical $\text{NaI}(\text{Tl})$ crystals. An example of a spectrum recorded in a cubic block made of building bricks (side: 1.5 m) available at the CRP2A laboratory (Bordeaux) is given in Fig. 2. However, this probe has the disadvantage of a relatively high background (Fig. 2), due to the presence of the ^{138}La isotope in the crystal lattice which generates γ - rays at 1436 and 789 keV, this second emission following a beta decay (end-point energy: 255 keV) that induces counts in the 789-1044 keV range. Thus, in the background spectrum, one also notices the presence of a line at 1461 keV, probably due to the

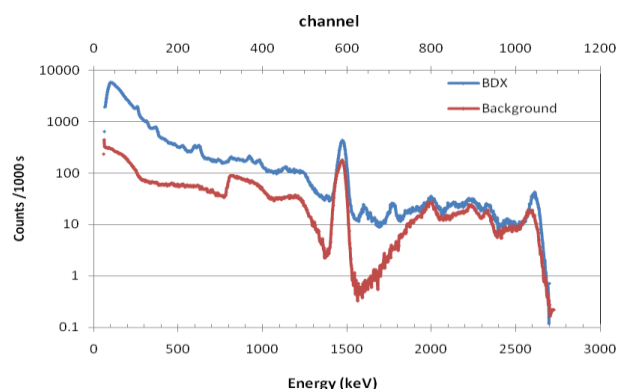


Figure 2: Time-normalized spectra (1000 s) recorded with a LaBr_3 probe placed in the block of bricks available at CRP2A (BDX- gamma dose rate = $2010 \pm 35 \mu\text{Gy/a}$) and in a lead housing (Background). High resolution gamma spectrometry performed on bricks used for building the CRP2A block allowed determination of their average radioisotopic contents: $U(^{238}\text{U}) = 4.27 \pm 0.68 \text{ ppm}$, $U(^{226}\text{Ra}) = 4.10 \pm 0.14 \text{ ppm}$, $\text{Th} = 13.7 \pm 0.3 \text{ ppm}$, $\text{K} = 3.50 \pm 0.05\%$. Note that the Y-scale is logarithmic.

summation of gamma rays of 1436 keV and X-rays following electron capture, as well as peaks related to the Th-series.

Counts were performed with this probe in the following Clermont reference rocks: C347, C341, PEP, LMP, MAZ and GOU, as well as in the Bordeaux block of bricks in order to get a point at $\sim 2000 \mu\text{Gy/a}$. As each spectrum is a mixture of γ - rays coming from the ^{40}K and U- and Th-series, we analyzed the spectra by applying two threshold techniques (Guérin and Mercier, submitted). With the first technique, the total number of pulses above a fixed threshold was accumulated and counted. This threshold value was determined with the Geant4 code simulating a LaBr_3 cell (encapsulated in a 1 mm thick duraluminium layer) placed in infinite media. These media had various compositions similar to sediments rich in carbonates, silicates, organic materials or lavas; the different radio-emitters - ^{40}K and those of the U- and Th-series- were distributed uniformly. According to these Monte-Carlo simulations, the number of counts detected per unit time by the LaBr_3 cell above an energy of 300 keV (ΣNi , $E > 300 \text{ keV}$), normalized to $1 \mu\text{Gy/a}$, is independent of whether the γ -rays originated from K, U or Th, and this value was then used as the low threshold. A high threshold of 2800 keV was set in order to eliminate the cosmic contribution to the counts (see Prescott and Clay, 2000). Fig. 3 shows the total count between 300 keV and 2800 keV as a function of the

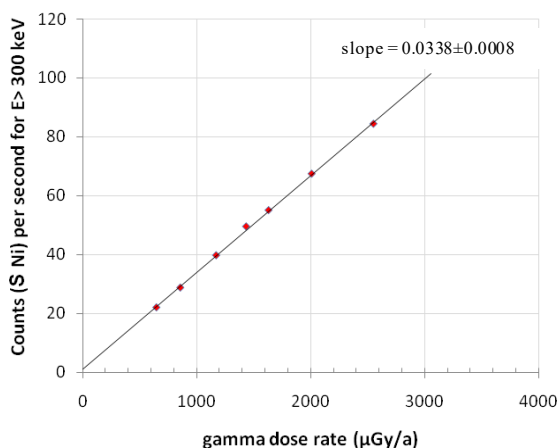


Figure 3: Net counts per second (ΣNi for $E > 300$ keV) deduced from measurements in the Clermont reference rocks and in the Bordeaux block of bricks as a function of the gamma dose rate (see values in Table 3). The upper discrimination level was fixed at 2800 keV, in order to eliminate the counts due to cosmic rays. Notice the good linearity and that the intercept is compatible with 0.

gamma dose rate, indicating that 0.0338 ± 0.008 counts per second for a $1 \mu\text{Gy/a}$ dose rate are detected with this probe.

The analysis of the same simulated data indicated that above 165 keV, the sum of the energy per unit time i.e. $\Sigma Ni \cdot Ei$ (which is, for each channel, the product of the number of counts in this channel with the corresponding energy) is also independent when normalized to $1 \mu\text{Gy/a}$, of the origin of the gamma-rays. In applying this second threshold technique, a larger part (about twice in counts number) of the recorded spectrum is used, which improves the counting statistics used for the dose rate determination. Moreover, Guérin and Mercier showed that this technique is less sensitive than the previous one to the repartition of the gamma dose rate between ^{40}K and the U- and Th-series. The same Geant4 simulations indicated that this technique is also nearly insensitive to the composition of the medium. With this second technique, a good linearity was found between the signals ($\Sigma Ni \cdot Ei$) and the gamma dose rates (Fig.4).

In situ TL dosimetry using the reference rocks

Verification of the consistency of the dose rate data

A campaign of TL dosimetry was especially devoted to check the internal consistency of the dose rate data (Table 3). For that purpose, powdered $\text{Al}_2\text{O}_3:\text{C}$

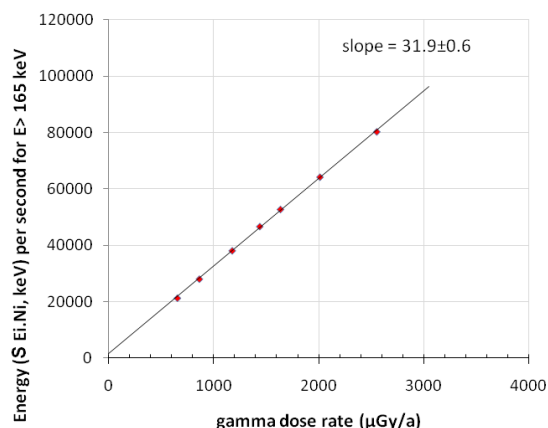


Figure 4: Time-normalized signal ($\Sigma Ni \cdot Ei$ for $165 \text{ keV} < E < 2800 \text{ keV}$) deduced from measurements in the Clermont reference rocks and in the Bordeaux block of bricks as a function of the gamma dose rate. The background was subtracted after time normalization.

(provided by Landauer Inc., Stillwater Crystal Growth Division) was used (grain size 200-315 μm). The Clermont laboratory routine dosimeter consists of a stainless steel tube (1.5 mm thick, 0.25 cm^3 of capacity) completely filled with the zeroed powder. The cap is held in place by a heat shrinkable tube, slightly longer than the steel tube (+ 1 cm at both ends). When in place and very hot, the shrinkable tube is pinched at both ends so as to form a water proof bag around the steel tube, in the form of a candy wrapping.

Such dosimeters were inserted in the holes for a few months and afterwards they were measured in the laboratory, all at the same time. The intensities of the TL peaks were plotted against the known dose rates (Fig. 5). No correction was applied to the results, because possible undesirable effects, such as self dosing and fading, would be the same for all the dosimeters and therefore should not affect the linearity of the curve. However, this is not true for attenuation by the walls of the tube, which depends on the gamma spectrum – that is the respective proportions of U, Th and K in the rocks – and on the composition of the rock (see e.g., Valladas, 1982; Faïn et al., 1985). The exact attenuation in the different media for the given configuration has not been computed yet. It can be expected from preliminary results that the difference of attenuation between the samples is in the range 0 – 3 %.

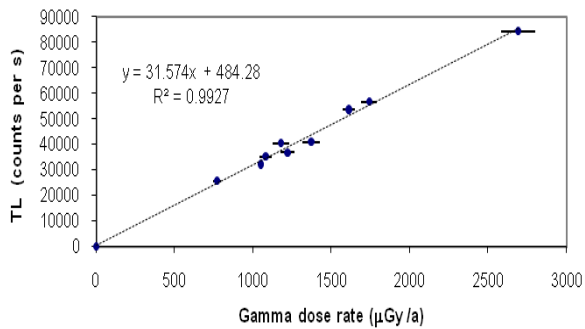


Figure 5: Plot of TL signal vs dose rate for 8 reference rocks.

A good correlation between TL and estimated dose rates was obtained (Fig.5), thus proving the validity of the data.

TL dosimetry

Routine methods for evaluating the dose acquired in situ by a TL dosimeter imply the use of a calibrated radiation-source (X, beta or gamma) for getting the correspondence: TL vs dose. Conversion of the measured equivalent dose in terms of in situ annual dose may require application of correction factors such as those evoked above for fading or self-dose; such corrections are routinely made by certain laboratories. Moreover, it necessitates a precise knowledge of the dose rate delivered by the laboratory source. So, inevitably, errors and uncertainties accumulate in the conversion. To overcome such problems, the Clermont TL group proceeds as follows.

When a set of dosimeters is to be placed in sites to be dated, 3 more dosimeters are prepared and placed in 3 of the 8 reference boreholes at the same time. After the dosimeters have been collected months later, all the phosphors are measured at the same time. Then, the TL intensities are plotted vs annual dose for the three known dosimeters. The dose rates in the different measured sites are then obtained by a simple interpolation (Fig.6). The overall uncertainty (systematic + statistical) on the result is estimated at 4.5 % of the annual radiation dose. The 3 reference rocks that have been chosen are C341, C347 and PEP. The advantages of choosing these rocks are: (i) the representative points on the initial experiment (see Fig.4) are on the mean regression straight-line (least squares method), meaning that the dose rates have been correctly evaluated for those 3 holes; (ii) the dose rates are significantly different from each other, allowing exploration of a large range of dose rates and, (iii) the sites are the most convenient, being the closest to the laboratory.

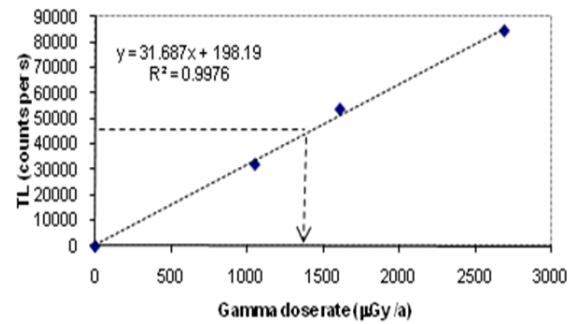


Figure 6: Plot of TL signal vs dose rate for 3 selected reference rocks (C341, C347 and PEP) based on a different campaign of measurements than the one for Fig.5. The dotted line shows the determination, by interpolation, of the annual dose for a dosimeter placed in a site to be dated.

Discussion of the method

The method offers advantages that have already been mentioned: several possible sources of error with the standard techniques have no effect here because they are the same for all the dosimeters and they are automatically corrected for by the interpolation. The method avoids the use of a laboratory source, with the relevant difficulties (authorization and calibration). Moreover, the number of TL (or OSL) measurements is limited: for N dosimeters, the total number of useful series of measurements is N+3 only (a "series" corresponds to the several measurements necessary for reducing statistical uncertainty for a given sample). Additionally, there is no need to measure the background (noise) or to worry about possible spurious signal.

However, the drawback of the method is that the sites of application must not be too far away from the laboratory. For remote sites, it is necessary to introduce complementary measurements for evaluating the travel dose; in any case, the in situ duration must be long enough for the corresponding dose to be significantly higher than the travel dose. Improvements of the method could consist of: (i) using a housing that would induce less dependence of the dose acquired by the TL phosphor on the composition of the measured medium and (ii), evaluation of the attenuation for a given medium with, e.g., a Monte Carlo code. Note that this applies to the standard methods too.

Conclusions

The reference rocks established around the Clermont laboratory can be considered as a convenient tool for various dosimetric experiments. The accuracy and precision of the data published in the present paper

can still be improved by new independent measurements, either in the boreholes or in the assessment of the nuclide content of samples from the cores.

Acknowledgements

We are grateful to Professor Martin Aitken for revision of the manuscript and useful comments.

References

- Adamic, G., Aitken, M.J. (1998). Dose-rate conversion factors: update. *Ancient TL*, **16**, 37–50.
- Aitken, M.J. (1985). *Thermoluminescence dating*. Academic Press, London.
- Bowman S.G.E. (1976). *Thermoluminescent dating: the evaluation of radiation dosage*. Unpublished D.Phil. thesis, Faculty of Physical Sciences, Oxford University.
- Faïn, J., Erramli, H., Miallier, D., Montret, M., Sanzelle, S. (1985). Environmental Gamma Dosimetry using TL dosimeters: efficiency and absorption calculations. *Nucl. Tracks Radiat. Meas.*, **10**, 639-649
- Faïn, J., Miallier D., Montret, M., Pilleyre, T., Sanzelle, S., Soumana, S., Bechtel, F., Guibert, P., Schvoerer, M., Vartanian, E., Mercier, N., Valladas, H., Bahain, J.J., Falguères, C., Tripier, J., Joron, J.L. (1997). Inter-comparisons dosimétriques dans le cadre de la datation par thermoluminescence et par résonance paramagnétique électronique: validation de milieux naturels témoins de la région de Clermont-Ferrand, Puy-de-Dôme, France. *Revue d'Archéométrie*, **21**, 29-34.
- Guérin, G., Mercier, N. (submitted) Determining gamma dose rates by field gamma spectroscopy in sedimentary media: results of Monte Carlo simulations. *Radiation Measurements*
- Miallier, D. Erramli, H., Faïn, J., Sanzelle, S. (1988). Doserate measurement by the enclosure method using Al₂O₃ TL dosimeters. *Nucl. Tracks Radiat. Meas.*, **14**, 193-197
- Murray, A.S. (1982). *Environmental radiation studies relevant to thermoluminescence dating*. Unpublished D.Phil. Thesis, Faculty of Physical Sciences, Oxford University.
- Prescott, J.R., Hutton, J.T. (1988). Cosmic ray and gamma ray dosimetry for TL and ESR. *Nucl. Tracks Radiat. Meas.* **14**, 223-227
- Prescott, J.R., Hutton, J.T. (1994). Cosmic ray contributions to dose rates for luminescence and ESR dating: large depths and long-term variations. *Radiation Measurements*, **23**, 497-500.
- Prescott, J.R., Clay, R.W. (2000). Cosmic ray dose rates for luminescence and ESR dating: measured with a scintillation counter. *Ancient TL* **18**, 11-14.
- Rhodes, E. J., Schwemmer, J.-L. (2007). Dose rate and radioisotope concentrations in the concrete calibration blocks at Oxford. *Ancient TL*, **25**, 5-8.
- Sanzelle, S., Erramli, H., Faïn, J., Miallier, D. (1988) The assessment of gamma dose rate by gamma ray field spectrometer. *Nucl. Tracks Radiat. Meas.*, **14**, 209-213
- Soumana, S. (1993). *Amélioration des techniques de dosimétrie appliquées à la datation par thermoluminescence*. Unpublished Thesis, Université Blaise Pascal, Clermont-Ferrand, France.
- Soumana, S., Faïn, J., Miallier, D., Montret, M., Pilleyre, T., Sanzelle, S., and Akselrod, M. (1994) Gamma and enclosure dosimetry for TL/ESR dating with the new Al₂O₃:C TL dosimeter. *Radiation Measurements*, **23**, 501-505.
- Valladas, G. (1982). Mesure de la dose γ annuelle de l'environnement d'un site archéologique par un dosimètre TL, *PACT* **6**, 77-85.

Reviewer

J.R. Prescott

Referee Comments

The major thrust of the paper is the idea of using boreholes in massive rocks as defined locations for dose rate calibration. Both gamma-ray spectrometry and in situ TL dosimetry are described. The idea is a good one and very useful if they are not too far from home, as the authors state. Many laboratories have access to pads of known composition with added K, U and Th. Some have substantial blocks, buried underground. The use of natural features avoids the need to make your own pads. Although it requires more work, the procedure described for in situ TL dosimeters and to minimise sources of error will appeal to those who do not have "in house" radiation facilities.

The use of the relatively new LaBr₃ (Ce) scintillation counters, as described in the text, is satisfactory for total gamma ray dosimetry. It must be noted however that the manufacturers explicitly do not recommend them for low level counting. In the present context this would be the case if concentrations of K, U or Th were being measured individually.

Annex 1

List of the persons who contributed to the assessment of the nuclide content and/or gamma dose rate in the reference blocks.

Laboratory	Person	Method
Centre de Recherches en Physique Appliquée à l'Archéologie, CRP2A, Université de Bordeaux 3.	P. Guibert, N. Mercier	Gamma spectrometry (Hp- Ge detector), field gamma-probe.
Laboratoire des Sciences du Climat et de l'Environnement, LSCE, Gif-sur-Yvette.	N. Mercier, H. Valladas	TL, field gamma-probe.
Institut de Paléontologie Humaine, IPH Paris	J.J. Bahain, C. Falguères	Gamma spectrometry (Hp- Ge detector)
Laboratoire Pierre Sue, CEA, Saclay	J.L. Joron	NAA
Laboratoire Magmas et Volcans, Clermont-Ferrand.	M. Condomines	ICP-MS, alpha spectrometry
Laboratoire d'analyses et mesures, CRN, Strasbourg	J. Tripier	TL
Laboratoire de Physique Corpusculaire, LPC, Clermont-Ferrand	J. Faïn, H. Erramli, D. Miallier, T. Pilleyre, S. Soumana, S. Sanzelle	Gamma spectrometry (Hp- Ge detector), TL
Centre de Recherches Pétrographiques et Géochimiques, CRPG, Vandoeuvre-lès-Nancy		ICP-MS
Hokkaido University of Education, Japan.	Y. Ganzawa	NAA

The “AGE” program for the calculation of luminescence age estimates

Rainer Grün

Research School of Earth Sciences, The Australian National University, Canberra ACT 0200, Australia

(Received 19 November 2009; in final form 21 November 2009)

Abstract

The supplementary ZIP file of this paper contains the AGE program, which can be used for luminescence age calculations of clastic sediments. This paper outlines the use and limitations of this program.

Introduction

At the recent APLED2 meeting in Ahmedabad, it was brought to my attention that quite a number of colleagues still use the DOS-based “AGE” program for the calculation of luminescence ages. This program was actually never made widely available nor did it have any explanatory notes; this paper will address these issues.

The supplementary ZIP file¹ of this paper contains the AGE program, which is written in Quick Basic, a DOS based language. Note that some DOS commands are not supported by Windows XP and Vista, and that Vista users will require DOS emulation software in order to run the program. Particularly, there are problems associated with printing the results. AGE uses the “lprint” command, which is not supported by USB printers. The program is mainly driven by function keys.

The program is based on dose rates from Adamiec and Aitken (1998), beta attenuation factors from Mejdahl (1979), alpha attenuation factors from Bell (1980), and cosmic dose rates from Prescott and Hutton (1988, 1994).

Data input

In the following description, input fields are written in italics.

When the software package is opened, the left side inputs refer to internal dose rate parameters and the right side to external ones. *BETA ATTENUATION*

toggles between the calculation of external beta attenuation / self absorption based on the grain size, layer removed and internal infinite matrix dose rate (the external dose rate is then set to zero). *INT. ALPHA / INT. BETA* allows the input of calculated or measured alpha and beta dose rates. The associated *av. α/β -SELFIRR* toggles the use of average internal absorption factors to the supplied dose rates (i.e. if these are infinite matrix dose rates, the absorption factors may have to be applied).

The external sediment values are used for the calculation of the external α and β dose rates. *FOR α/β IRR. ONLY* toggles the addition of the gamma dose rate calculated from the sediment data. Similar to the internal dose rates, external alpha and beta dose rates can be added with or without the calculation of average attenuation factors. In addition, an external gamma dose rate can be added with or without consideration of water attenuation.

The cosmic dose rate attenuation is calculated for average sediment densities of 2 g.cm^{-3} (hard and soft component, after Prescott and Hutton 1988, 1994, see also discussion in Grün 1994). A zero input leads to a zero cosmic dose rate. A surface dose rate is calculated by a non-zero value, e.g. 0.001. Other densities can be calculated by scaling the depth. The cosmic dose rate is only calculated to a depth of 25m, below that, the formula used would give erroneous results. Latitude and altitude corrections (Prescott and Hutton 1994) are not carried out. If these are required, they have to be manually adjusted in the *EXT. GAMMA* entry. The cosmic dose rate is added to the external gamma dose rate.

Text files (with an .AGE extension) with the data are saved in the specified directories. As this is a DOS file, any sample name cannot be longer than 8 characters.

When reading existing data files, or using the F2 function key after the calculation of results, data

¹ The ZIP file associated with this paper can be obtained from the Ancient TL web site at www.aber.ac.uk/ancient-tl/issue27_2/age.zip

entries can be revised using arrow keys and “Enter”. A straight second “Enter” restores the previous value, any other input leads to a revision of the previous value. Results are printed using the “ESC” key.

Error calculation

The mean dose rates are calculated from all mean values. The effect of each error input is calculated for the total dose rates as well as all given dose rate components. It is explicitly assumed that the errors are linear within the error range. Note that the errors of the alpha, beta and gamma dose rates do not necessarily add up in quadrature to the error in the total dose rate, because some of the errors in the partial dose rates are highly correlated. The age estimate and its error are not rounded. Please make sure to report only relevant digits.

A program for the calculation of ESR age estimates on tooth enamel is available from the Quaternary Geochronology web-site (see Grün 2009).

Acknowledgment

I am grateful to Ashok Singhvi for inviting me to APLED2 where discussions with various colleagues led me to write this paper. I am grateful to the Institut des Sciences humaines et sociales du CNRS, Bordeaux, and the Laboratoire d'Anthropologie des populations du Passé, Université de Bordeaux I, for their kind hospitality in the writing-up stage of this manuscript.

References

- Adamicc, G., Aitken, M.J. (1998). Dose-rate conversion factors: update. *Ancient TL* **16**, 37-50.
- Bell, W.T. (1980). Alpha dose attenuation in quartz grains for thermoluminescence dating. *Ancient TL* **12**, 4-8.
- Grün, R. (1994). A Cautionary Note: Use of 'water content' and 'depth for cosmic dose rate' in the AGE and DATA programs. *Ancient TL* **12**, 50-51.
- Grün, R. (2009). The DATA program for the calculation of ESR age estimates on tooth enamel. *Quaternary Geochronology* **4**, 231-232.
- Mejdahl, V. (1979). Thermoluminescence dating: beta-dose attenuation in quartz grains. *Archaeometry* **21**, 61-72.
- Prescott, J.R., Hutton, J.T. (1988). Cosmic ray and gamma ray dosimetry for TL and ESR. *Nuclear Tracks and Radiation Measurements* **14**, 223-227.
- Prescott, J.R., Hutton, J.T. (1994). Cosmic ray contributions to dose rates for luminescence

and ESR dating: large depths and long-term time variations. *Radiation Measurements* **23**, 497-500.

Reviewer

Geoff Duller

Single grain OSL analysis: A discussion of how to clean and check single-grain discs

A. D. Davies and D. C. W. Sanderson

SUERC, East Kilbride, G75 0QF, UK

(Received 15 September 2009; in final form 7 December 2009)

Abstract

We compare possible methods to remove grains from single grain discs including heating, tapping, vibration in a sieve shaker and use of an ultrasonic bath. These methods are quick, simple and effective at removing smaller grains or those that have become stuck as a consequence of settling during pre-heating. Holders for single grain discs to facilitate thermal and vibrational cleaning approaches have been designed and manufactured. Heating and tapping seem to be useful additional techniques for cleaning single grain discs, resulting in insignificant residual sensitivity in the majority of cases.

Introduction

Optically stimulated luminescence (OSL) analysis of single grains has proven to be a valuable means of enhancing luminescence dating. It has been shown that there is significant variability in luminescence properties and sensitivity between grains (Duller et al., 2000; McCoy et al., 2000). With single-grain analysis it is possible to investigate such behaviour, and importantly, attempt to separate components within complex mixtures (e.g. Thomsen, 2004) or identify grains that have been heated in a fire (Moska et al., in press). However, the sensitivity of single grains of quartz frequently leaves many observations at, or close to, statistical detection limits for photon counting. Thus it is extremely important to check the blank levels of cleaned discs between runs, and to carry forward realistic estimates of detection limits into the analysis. In this paper we look briefly at how to clean single grain discs from the Risø DA-20 system, using blank scans in the reader and scanning electron microscopy to evaluate performance. The Risø guide (2007) suggests that the safest cleaning method is an ultrasonic treatment with water or alcohol. Here we have also evaluated thermal and vibrational approaches with promising results.

After each cleaning process was applied, discs were analysed in three ways to check for residuals. The disc was first observed under an optical microscope, which was rapid but did not provide enough detail to fully confirm that there were no grain fragments. This

detail was provided by looking at the disc under a scanning electron microscope (SEM). Finally, to check for remaining OSL signals a “disc cleaning check” was carried out on the Risø single grain reader. This comprised application of a fixed beta dose of roughly 10 Gy (supplementing the signal induced by electron beam irradiation under SEM examination) followed by preheating to 160°C (at 5°C/s and held for 10 s) and an OSL measurement for 2 s. Data from the OSL check were classified on the basis of the number of times that observed net OSL signals exceeded estimated poisson uncertainties. The signal from the first 0.5 seconds of optical stimulation was integrated and signal during the last 0.5 seconds was used for background subtraction to calculate the “net” signal. The detection limits, applicable to subsequent runs, for each disc and hole were then defined as the mean value plus three standard deviations. Even unused discs and cleaned discs produced a small, but detectable, signal (Fig. 1). To ensure that each single grain disc could be subsequently tracked, a number was engraved on its back.

Discussion of methods

Twenty-six discs were examined using the methods outlined below. These discs had previously been used to measure quartz from a range of sample sites (Orkney, Italy and Sri Lanka) and all had been sieved to 150–250µm diameter.

Cold tapping

The majority of grains were found to be easily removed by “cold tapping” – tapping the discs upside down followed by brushing and spraying with compressed air. This only removed all the grains on three discs out of 17 (there were 9 discs for which this method was not used) but for the discs that were not completely cleaned, only between one and ten grains remained. The removal of the loose smaller grains prevented any grains from returning to holes as well as isolating these stuck grains. To improve the cleaning process, a single grain disc holder was designed (Fig. 2) which holds the discs upside down above a pit for collecting fallen grains and, when the

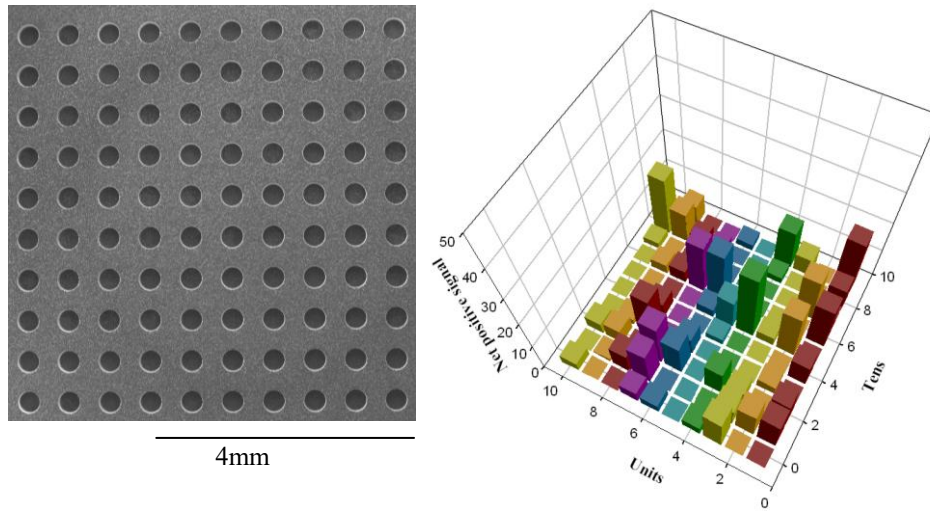


Figure 1: An SEM picture of a cleaned disc and the net OSL signal (photon counts) produced by that disc for each hole.



Figure 2: Single grain disc holders to help with the cleaning process and to store the discs.

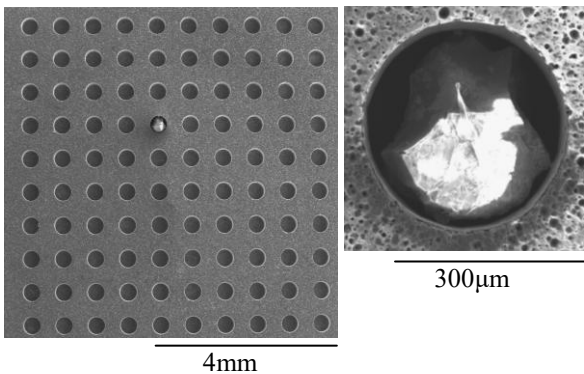


Figure 3: A grain wedged in a hole because of two points of contact on opposite sides of the hole (note the charging on the grain which has occurred because the discs were not coated).

discs are clean, prevents them from being contaminated. Furthermore, the holder can be used for all the different cleaning methods and discs can safely be stored with grains in.

Hot tapping

Some grains are the correct size and shape to become wedged in the holes on the single grain discs (Fig. 3). It was thought that these grains may have become wedged in the hole as a result of the hole expanding during preheating in the Risø Reader. If the disc is preheated to 220°C (a temperature rise of roughly 200°C), this corresponds to an increase of 1.39µm in the diameter of the hole since the coefficient of thermal expansion for aluminium is $23.1 \times 10^{-6} \text{ K}^{-1}$. This may cause grains to settle into positions which trap them when the holes contract on cooling. Therefore, theoretically, heating the disc upside down to a temperature above the preheat temperature, such as 400°C, and giving it a sharp tap should remove grains that had become stuck through that process. This method was quite successful at dislodging large grains such as the one shown in Fig. 3. All but eight discs were fully cleaned from only using cold tapping and one to three cycles of hot tapping. Statistics of the photon count from a disc as it passed through the methods outlined above are given in Table 1.

Shaking

It was noticed under the SEM that the sides of the holes were not completely smooth (Fig. 4) and may also cause grains to have a difficult path out of the hole even when it has been expanded using heat in the “hot tapping” method.

	Number of holes with signals significant at 3σ	Mean net signal of the holes with insignificant signals (photon counts)	Largest net signal (photon counts)
Before cleaning	24	1.6	4913
After "cold tapping"	13	-1.0	2336
After "hot tapping"	2	-1.8	30
Mean of all 25 cleaned discs	3.3 ± 0.4	-0.7 ± 0.3	45.3 ± 6.2

Table 1: An example of what happened to one of the discs as it was cleaned using the methods outlined above. The final row gives statistics of the 25 cleaned discs (not including the one disc that had two grains remaining in it) compiled from the "disc cleaning check" runs.

Shaking the discs while they were still hot was attempted as an enhancement to the "hot tapping" method so an adapter to fit onto a Fritsch *pulverisette analysette laborette* laboratory sieve shaker was manufactured (Fig. 5). This holds three of the single grain disc holders (Fig. 2) which can be preheated in an oven. This method appeared reasonably successful, and can be readily incorporated into standard procedures. At present it is unclear whether the performance exceeds that from "hot tapping" alone.

Ultrasonic treatment

For four discs, hot tapping had left one grain stuck in each disc. To try a more vigorous method of shaking the grains out of the hole, an ultrasonic treatment in water followed by drying using methanol was employed as suggested in the Risø Guide (2007). For three of the discs, the ultrasonic treatment removed the final grain. However, for the fourth disc, another cycle of heating and ultrasonic treatment was required to remove that grain implying that a combination of the methods enhances the removal process.

To ensure that ultrasonic treatment was not a sufficient method on its own, three discs were first cleaned using the ultrasonic bath and then photographed under the SEM. An average of 5 grains remained in each disc and these grains were removed by the subsequent heating (Fig. 6).

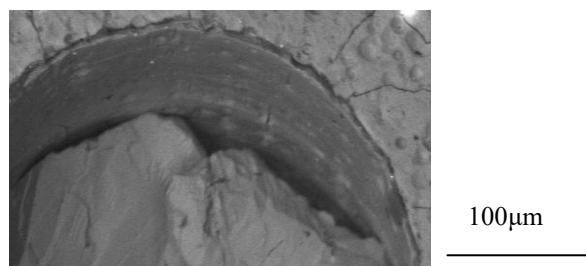


Figure 4: An SEM image of the side of a hole where the side shows some roughness.



Figure 5: An adapter for a laboratory sieve shaker which holds 3 single grain disc holders.

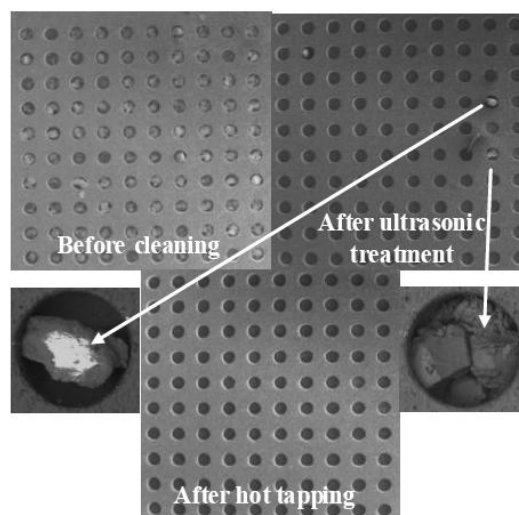


Figure 6: SEM photographs of a disc that was first cleaned using ultrasonic treatment and then by hot tapping showing some of the grains that were only removed after heating

The combination of ultrasonic treatment and heating has not been able to clean the final disc which contains two grains stuck in a hole (Fig. 7). It is

thought that these two grains are wedging each other into the hole.

Summary and Conclusions

The last line in Table 1 summarises the overall performance achieved in cleaning 25 discs using all methods. This does not include the one disc, from the original 26 examined, that was not completely cleaned (Fig. 7). From this initial study, a combination of heating and ultrasonic treatment was found to be very effective at cleaning all but one hole from a total of 2600 holes examined.

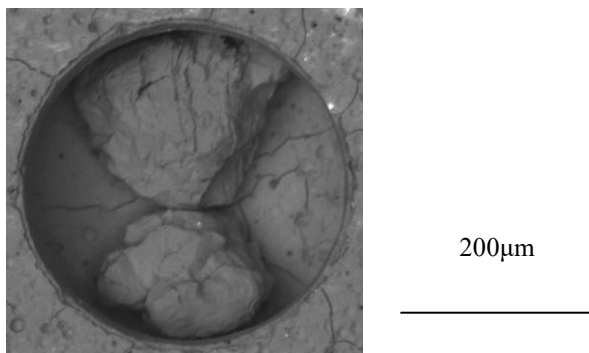


Figure 7: The grains that have not been dislodged from the hole of one disc.

The cleaned discs gave little statistically significant residual signal and no grain fragments could be seen under the SEM. Further work is required to enhance these cleaning methods to ensure that reused discs have been reliably cleaned and contain little residual signal that could contaminate further results.

Acknowledgements

We would like to thank SUERC for supporting this project as well as Simon Murphy for his help with manufacturing the disc holders and sieve shaker adapter. Rachael Ellen also provided help and advice that was greatly appreciated.

References

- Duller, G.A.T., Bøtter-Jensen, L., Murray, A.S. (2000) Optical dating of single sand-sized grains of quartz: sources of variability. *Radiation Measurements* **32**, 453-457.
- McCoy, D.G., Prescott, J.R., Nation, R.J. (2000) Some aspects of single-grain luminescence dating. *Radiation Measurements* **32**, 859-864.
- Moska, P., Murray, A.S., Bluszcz, A. (in press) Luminescence properties of single grain quartz to determine the history of a sample from the Sahara Desert. *Quaternary Geochronology*.

Risø National Laboratory (2007) Guide to "The Risø Single grain laser OSL system".

Thomsen, K.J. (2004) *Optically stimulated luminescence techniques in retrospective dosimetry using single grains of quartz extracted from unheated materials*. PhD thesis, University of Copenhagen

Reviewer

G.A.T. Duller

Referee Comments

Ensuring that single grain discs are clean prior to measurement is essential to obtain reliable OSL data. As all users of single grain systems will know, cleaning these discs is a constant challenge. The new methods described here are a valuable addition to those available to practitioners.

Thesis Abstracts

Author: Gloria I. López
Thesis Title: The late Quaternary evolution of the Apalachicola barrier island complex, north-east Gulf of Mexico, as determined from optical dating¹
Grade: Ph.D.
Date: September 2007
Supervisor: W. Jack Rink
Address: School of Geography & Earth Sciences, McMaster University, 1280 Main Street West, Hamilton, Ontario, Canada

Optically stimulated luminescence (OSL) studies of clastic-rich coastal environments have been increasingly the focus of attention, mostly over the past five years, due to the improvement of protocols used to obtain reliable and accurate optical ages on minerals such as quartz. Using 55 quartz-separate samples extracted from at least two different depth intervals on sediment cores (long vertical and short horizontal) retrieved from multiple beach/dune ridges that decorate four Holocene coastal barriers and a Pleistocene lower mainland, the supra-tidal evolution of the western portion of the Apalachicola Barrier Island Complex, on the NE region of the Gulf of Mexico, has been re-evaluated. This study not only provides new reliable OSL ages for the region but also addresses the feasibility of a) quantifying rates of coastal aggradation and progradation; b) interpreting the temporal chronology of the coastal geomorphology; and c) constraining the results with other geochronometric data available at a more precise level (e.g. inter-correlations with accurate [x,y,z] parameters).

OSL results show equivalent doses (D_e) ranging between 0.01 ± 0.00 and 52.28 ± 1.26 Gy, associated to samples linked to both wind- and water-lain processes, depicting the two principal components of these ridges: a most probable swash-built ridge base and an aeolian cap. The optical ages obtained range from 22 ± 4 to $154,200 \pm 10,400$ years ago (based on 2004 to 2006 datum), representing terminus ante quem ages of formation of the base of the ridge and the ages of the aeolian component at that particular depth. The sedimentary deposits hosting the cores collected show minimal contents of Uranium and Thorium ($\ll 4$ ppm with an average of 0.5 ppm). The

Potassium content seems to be more linked to temporal variations (i.e. different stages of evolution of the barrier islands) than to geographical position relative to the Apalachicola River mouth.

D_e distribution analyses show that frequency histograms coupled with cumulative frequency (%) curves and radial plots should be used together to better evaluate the overall behaviour of the distribution. For most of the samples OSL-dated for this research, one or two outliers (i.e. aliquots outside $\pm 2\sigma$) were present upon analysis of the D_e distribution, but excluded from the final D_e calculation used to compute the optical age of each sample. Skewness coefficient ranges were determined and skewness values were calculated to quantify the degree of symmetry of the D_e distribution for each sample. This parameter was used to assess the analytical error to be associated with each final D_e value, as well as the heterogeneity or homogeneity of the dose within each sample and see any indications of possible incomplete zeroing or biogeoturbation. Moreover, and associated with the latter, the use of smaller aliquots (e.g. 3 and 1 mm mask sizes) was also implemented to detect if the samples had undergone any significant post- or pre-depositional disturbance. None was found; rather, analyses show that with decreasing mask size, an increasing resolution in the D_e distribution was obtained where the values obtained for the larger aliquots (i.e. 8 and 5 mm mask size) were encompassed within those obtained for the smaller aliquots (i.e. 3 and 1 mm mask size).

This dissertation presents the first assessment of supra-tidal coastal evolution using optical ages to determine both the vertical accretion and lateral progradation rates throughout different segments of the coastline. The multidirectionality, patterns and truncations shown by the hundreds of beach and dune ridges and ridge sets demonstrate the morpho- and hydro-dynamic complexity of these coastal barrier systems, located on the apex of the Floridian Panhandle. Assessments of such morphological characteristics as well as detailed analyses of air-photographs, satellite imagery, ancient nautical and topographic charts/maps, and previous studies were also incorporated in this research to better constraint the proposed Late Holocene spatial-temporal history of this ~ 60 km-long coastal complex perched on the NE corner of the Gulf of Mexico. Six major time intervals were differentiated with the chronological evolution of these barrier islands since the last ~ 4,000 years.

¹ The full text of this thesis is available online at www.aber.ac.uk/ancient-tl

Author: Damian Steffen
Thesis Title: Quaternary accumulation and erosion of sediment in the drainage basins of the western escarpment of the Andes of Peru: The role of climatic variations
Date: December 2008
Supervisors: Frank Preusser, Fritz Schlunegger
Address: Institute of Geological Sciences, University of Bern, Switzerland

This thesis investigates the role of climate on the formation of terraces and fans based on two case studies in southern Peru. Two valleys, the Pisco (~13.5°S) and Majes (~16°S) valleys that extend in an east-west direction from the Altiplano to the Pacific coast, and where terraces and fans are numerous, were investigated in detail. Both valleys are characterized by a dry climate along the coast and in the lower reaches and a semi-arid climate in the headwaters. In order to interpret the formation of the terraces and fans, it was essential to establish a detailed chronological framework, and for this study, this was done using luminescence dating. During the analysis of the luminescence samples, it became clear that the quartz OSL (optically stimulated luminescence) ages from terraces and fans underestimate the true depositional age. Deconvolution of OSL signals revealed that the fast component was not dominant in the luminescence signal and, in addition, determination of thermal lifetimes using pulse annealing showed that the medium component was thermally unstable, with both problems resulting in age underestimation. Testing suggested that the weak fast component and thermally unstable medium component may be related to the young sedimentary history of the quartz grains that are directly derived from weathered plutonic and volcanic rocks. Multiple cycles of bleaching, heating and irradiation of the quartz grains may improve their characteristics for luminescence dating. A possible solution to circumvent problems related to a thermally unstable medium component is to isolate the fast component. This was done using different approaches, including mathematical extraction as well as direct sampling of the fast component using a modified SAR (single aliquot regenerative) protocol. None of these techniques proved robust enough to allow its routine application to the dating of quartz from the Pisco and Majes valleys, and it was found preferable to use feldspar IRSL (infrared stimulated luminescence) instead. Extensive testing of feldspar IRSL was also

conducted after which it was successfully applied to date the terraces and fans. While anomalous fading is often seen to affect the feldspar signal, testing of this confirmed that it was not present for these particular samples.

IRSL dating of the terraces and fans in the Pisco and Majes valleys revealed that phases of sediment aggradation were contemporaneous with humid periods on the Altiplano. Aggradational phases occurred during the Ouki (~110-100 ka), Minchin (~55-40 ka), Tauca (26-15 ka) and Coipasa (12-8 ka) paleolake cycles. The sedimentologic and geomorphic data suggest that enhanced precipitation in the headwaters and middle part of the catchment resulted in increased erosion and transportation of sediment from the hillslopes into the channel network and towards the lower reaches. An imbalance between sediment supply from hillslopes, and sediment transport capacity of the receiving trunk stream, in combination with a decreasing river gradient and an increasing valley width beneath the knickzone most probably resulted in deposition of the sediment. Not only were the headwaters affected by this climate change but also tributary catchments and hillslopes in the lower reaches that are currently arid. There, controls on sediment discharge in the tributary systems and mechanisms driving fan construction were considered to be local. Due to the absence of vegetation cover, sediment discharge in the tributary drainage basins is very sensitive to changes in the rainfall pattern. A change towards a climate with a higher frequency of high-magnitude precipitation events most likely initiated the construction of fans. While the onset of erosion of previously deposited sediment cannot be directly inferred from the luminescence data, field evidence suggests that the erosion may have started in the later stages of a wet period as sediment availability on the hillslopes tapered off. We conclude that terrace and fan systems therefore record the combined effect of allo- and autogenic mechanisms initiated by a shift towards a more humid climate. Supply of sediment and formation of terraces and fans not only depends on climate and water discharge, but also to a large extent on the availability of unconsolidated material on hillslopes. Bedrock weathering, therefore, has presumably been the most important limiting process for terrace and fan construction, particularly in arid regions. This implies that the number of periods during which terraces and fans in the Majes valley were formed only provides a minimum estimate of climate cycles, and it is possible that further wet periods occurred that are not recorded in the sedimentary deposits where the time scale of climate change was shorter than the time required for weathering and the production of new sediment.

Author: Yu-Xin Fan
Thesis Title: A study on the evolution of the Jilantai-Hetao Megalake: focusing on optical dating of lakeshore sediments
Grade: PhD
Date: December 2008
Supervisors: Fa-Hu Chen, Hui Zhao and Charles G. Oviatt
Address: CAEP, MOE Key Laboratory of West China's Environmental Systems, Lanzhou University, Lanzhou 730000, P.R.China

The Jilantai Salt Lake is located in the southwestern part of the Jilantai-Hetao Basin, a Cenozoic fault basin to the north and northwest of the Ordos plateau and to the east of the Alashan plateau in western China. The Jilantai-Hetao basin is about 560 km long and 80 km wide. Most of the lake basin is now dry and covered by aeolian sand. A series of lakeshore remnants were found around the Jilantai Salt Lake, especially on its western bank. Altitudes of these shorelines are at 1080-1070m, 1060m, 1050m, 1044m and 1035m asl. It could be inferred that at the highest lake level stage, a huge lake, the Jilantai-Hetao Megalake, was developed to cover the Jilantai area and most of the Hetao Plain along the Yellow River at its square bend around the Ordos block. However, many questions remain unsettled. For instance, can this hypothesis be supported by geological and geomorphologic evidence? When and how was such a huge lake formed? Researches of above questions are of great importance to study the development of Ulan Buh and Kumbuqi Deserts, and the evolution of the Yellow River as well.

In this study, geomorphologic, sedimentary and biological evidence of the Jilantai-Hetao Megalake were summarized based on our previous studies. OSL dating of lakeshore sediments was studied in detail and the reliability of these OSL dates was discussed on the basis of luminescence chronology and the comparison with radiocarbon dating. A preliminary chronological frame of the paleolake's major shorelines was determined based on forty-nine OSL dates from a series of sediments on different shorelines. From analyzing the potential water sources to the huge lake, the probable formational mechanism of this huge lake was also discussed. The following main results were reached:

1) Geological and geomorphological evidence.

Barrier bar, wave-cut terrace and spit are the typical geomorphological evidence of the lakeshore in the Jilantai and Hetao area. Barrier bars are widely distributed in the Jilantai area, especially on the west

bank of the Jilantai Salt Lake. Lacustrine sediments and wave-cut terraces were found on the southern piedmont of the Langshan-Seertengshan-Daqingshan Mountains where was proved to be the north margin of the lake basin, and on the piedmont of Zhuozi Mountains east to the Wuda District, the south margin of the lake basin. Geomorphologic features of lakeshores were poorly preserved on the south bank of the Yellow River, but lacustrine deposits were found in several excavated sand quarries, for example in quarries east to Sanshenggong Bridge, in quarries southeast to Balagong Town in the western bend of the Yellow River, and especially in quarries near Shilazhao south to the Urad Qianqi which is on a sub-upleft of the basin. Spits are mainly distributed in the Jilantai area, for example, two typical spits are existed with specific geomorphological features at sites west to the Jilantai Salt Lake and seventy kilometers northeast to the Jilantai Town respectively. In addition, there is a delta at the west-south mouth of the lake basin to the east of the Wuda district, which was probably formed by the Yellow River inferred from geomorphological evidence. The exposed profiles on lakeshores have a general vertical prograding sequence. Shells of aquatic mollusk, such as *Corbicula*, *Radix* and *Gyraulus* were found in most of lakeshore sediments. These observations support that there was once a unified huge lake covering the Jilantai area and most of the Hetao Plain, referred to as the Jilantai-Hetao Megalake.

Based on spatial distribution of these shorelines and their altitudes in the Jilantai area, an area weakly influenced by tectonic movement, it was deduced that Jilantai-Hetao Megalake underwent three evolutionary phases as the Jilantai-Hetao Megalake phase with shorelines at altitudes 1080-1070m asl, the Jilantai-Hetao Main Lake phase with shorelines at altitudes of 1060-1050m asl and the Jilantai Paleolake phase with shorelines at altitudes of 1044-1035m asl.

2) Luminescence dating of the lakeshore sediments.

From profiles on different altitudes of shorelines, forty-nine OSL samples of different kind lakeshore sediments were collected. These samples were measured by using the OSL technique. For improving the reliability of OSL dating results of lakeshore sediments, the relationship between quartz grain-size and equivalent dose (D_e) values is studied from five littoral sediments samples. The creditability of all OSL results is discussed from D_e and dose-rate determination. And the reliability of these OSL dates is also validated through the comparison with radiocarbon dating in six profiles.

Lakeshore sediments were suggested to be potentially well-bleached suitable for OSL dating by the comparison of D_e in the 1990's. However, recent comparison of dating results from different

chronological methods has shown that the luminescence technique may underestimate the age of lakeshore sediments. To investigate the reliability of OSL dating of lakeshore sediments, five lakeshore samples in the Jilantai area were examined by comparing D_e values of quartz fractions in the size ranges of 63-90, 90-125, 125-150, 150-180, 180-250 and 250-300 μm in each sample. The D_e values were measured by using medium aliquots. There are two different relationships between D_e values and grain sizes of these samples. The first relationship is that the D_e values obtained from various grain sizes are in agreement within 1 delta errors. The second relationship is that D_e values are similar to each other for fractions between 125 and 300 μm , while the D_e value of the 63-90 μm fraction is 40~55% smaller than others. For example, the D_e values obtained for sample #3 are 20.15 ± 1.19 Gy, 19.80 ± 0.83 Gy and 20.93 ± 1.06 Gy for fractions of 90-125, 125-150 and 250-300 μm respectively, but are 10.79 ± 0.84 Gy for the 63-90 μm fraction. The second relationship can't be interpreted by previous studies of both dosimetry and heterogeneous bleaching. It is deduced for sample #2, #3 and #6 that fine particles (<90 μm) intruded after the dominant sedimentation. We compared the OSL ages of the 63-90, 90-125, 125-180 and 180-300 μm quartz fractions of sample #2 with a radiocarbon age from aquatic mollusk shells with both bivalves well preserved collected in the same lithologic layer (sample #7) in profile HS4, and results show that OSL ages from the 125-180 μm and 180-300 μm fractions are in the same time span very close to the radiocarbon dating result and those apparent ages of the 63-90 and 90-125 μm fractions are obviously 2800-3600 years younger than the radiocarbon dating result even when radiocarbon reservoir was considered. The comparison supports that fractions coarser than 125 μm yield more reliable burial ages, while the fraction finer than 90 μm yields underestimated ages for some lakeshore sediments from this arid region.

To obtain reliable chronological frame of the Jilantai-Hetao Megalake, OSL dating was applied to lakeshore sediments mainly for quartz fraction of 90-400 μm by using medium aliquots. The dating results show that the blue OSL signal of quartz fraction was near saturated in five samples. To these samples, IRSL dating was also carried out from k-feldspar fraction. The IRSL signals of these samples are unsaturated and their IRSL ages are about 15-50% younger than blue-OSL ages from quartz. For these five samples, OSL ages from quartz are used as the minimum age though their ages were potentially underestimated. The reliability of OSL results are also validated through the comparison with radiocarbon dating in six profiles. In three Holocene profiles, OSL dates are accordant with radiocarbon

ages of bulk organic matter or aquatic mollusk shell carbonates when radiocarbon reservoir was considered. In other three MIS 3 profiles, OSL dates of beach sand are also consistent very well with radiocarbon ages. For profile S39, the OSL age is 42.44 ± 4.20 ka with radiocarbon age of 41619~42241 cal a BP (two sigma deviation) of mollusk shells from the same lithologic layer. These comparisons indicate ages obtained from OSL dating of lakeshore sediments can be reliable as radiocarbon ages obtained from either bulk organic matter or aquatic mollusk shells, and that chronological frame can be established by means of OSL dating method.

The reliability of all OSL dates was summarized on the basis of above discussion. Finally, the chronological frame of the Jilantai-Hetao Megalake is reconstructed on these OSL ages, and the history of the megalake is recovered by the consideration of geomorphologic and geological evidence in this region. The OSL data demonstrate that the lake level came to rise from 120-100 ka or so, and subsequently a unified huge lake came into being, namely, the Jilantai-Hetao Megalake, covering the Jilantai Basin and almost the entire Hetao Basin before 60-50 ka. Then it gradually descended with its altitude remaining at about 1060-1050 m, and the lake still covered the Jilantai Basin and parts of the Hetao Plain. Thereafter the unified lake was separated into pieces. At around 10 ka ago, there were small separated lakes, possibly ponds in certain areas of Jilantai.

3) Formational mechanism of the megalake.

The changes of the unified Jilantai-Hetao Megalake into a dry lake basin indicate that the water system changed greatly in northern China. The cause of such a profound environmental change is an important issue that we are investigating through a number of research approaches. Based on field observations, we think it probable that the primary water source feeding the Megalake Jilantai-Hetao was the Yellow River. This assumption requires further testing, as does the possibility of contributions derived from other sources. We collected aquatic mollusk shells from littoral sediments at different altitudes around Jilantai and measured their strontium isotope compositions. $^{87}\text{Sr}/^{86}\text{Sr}$ ratios in shell carbonates are different between the high lake phase (~1080-1050m asl) and the low lake phases (~1044-1030m asl), with a small shift in average strontium ratios to more radiogenic values during the low lake phase. Based on regional hydrology and physical geography, we conclude that water from the Yellow River was the dominant water source supplying this mega lake. $^{87}\text{Sr}/^{86}\text{Sr}$ ratios of modern water samples suggest the Yellow River was the dominant water source during the high lake phase, but that the relative contribution of Yellow River water to the megalake was reduced,

and that the relative contributions of local precipitation and groundwater increased, during the low lake phase. Incision rates of the Yellow River indicate that the Ordos Plateau started to uplift rapidly on its western margin at about 120 ka with rapid uplift as a whole at about 100 ka. Lake levels in Jilantai and Hetao started to rise simultaneously as the rapid uplift of the Ordos Plateau. It is thus concluded that the Yellow River was possibly dammed by the rapid uplift of the Ordos plateau at the exit of the megalake, which resulted in the formation of the Jilantai-Hetao Megalake.

Author: Henrik Friis
Thesis Title: Luminescence spectroscopy of natural and synthetic REE-bearing minerals
Grade: PhD
Date: July 2009
Supervisors: Adrian Finch and Colin Donaldson (St Andrews), Terry Williams (Natural History Museum, London)
Address: School of Geography and Geosciences, University of St Andrews, Irvine Building, St Andrews, Fife, UK

This study investigates the photoluminescence (PL), cathodoluminescence (CL), radioluminescence (RL) and ionoluminescence (IL) of natural and synthetic minerals. The natural minerals (fluorapatite, leucophanite, meliphanite and zircon) are mostly from Ilímaussaq Alkaline Complex in South Greenland, Langesundsford in Norway and from different localities within Scotland. Synthetic fluorapatite (manufactured as part of the present study) and zircon doped with rare earth elements (REE) were used to compare single and multidoped materials. This study has shown that many of the generally accepted applications of luminescence are not as straightforward as often suggested by the current literature.

For example, the study demonstrates how site distribution of REE, based on luminescence, is greatly affected by the dopant level and structural changes, and that different conclusions can be drawn on the same sample depending on method applied. Furthermore, it is clearly demonstrated that using luminescence as a tool for quantitative trace element determination is not going to be a standard technique in the near future if ever. The two main findings supporting this conclusion are the nonlinear intensity decrease between different REE activators in the

same sample and a large variation between activators at the concentration at which self-quenching starts. In contrast to the general perception that luminescence related to REE is mostly independent of the host, this study has shown a strong interaction between host and REE activators.

This conclusion is supported by the change in the activator's coordination polyhedron observed with single-crystal and powder X-ray diffraction combined with full chemical characterisation. When combining the weak interaction between some REE with the strong host interaction this study has shown the potential for designing new types of colour tuneable and "white light" LEDs based on natural minerals. This study also reveals that zircon doped with Gd³⁺ and Eu³⁺ can potentially have quantum-cutting properties.

Author: Martina Demuro
Thesis Title: Optically stimulated luminescence dating of tephra-bearing deposits from eastern Beringia
Grade: PhD
Date: July 2009
Supervisor: Richard G. Roberts
Address: School of Earth and Environmental Sciences, University of Wollongong, Wollongong NSW 2522, Australia

Eastern Beringia (Alaska and the Yukon Territory) represents a unique high-latitude setting in that it has remained largely ice-free throughout the major global glaciations of the Quaternary. As a result, it contains extensive terrestrial palaeoenvironmental records in the form of perennially-frozen loess and loess-derived deposits, which span the last 3 million years. Numerous tephra horizons across eastern Beringia also provide invaluable chronostratigraphic markers that are capable of correlating regional stratigraphic sequences over large areas. These preserved records offer a unique opportunity to reconstruct detailed palaeoenvironmental, palaeoclimatic, palaeobiological and archaeological histories for this region. However, there remains a need to improve and expand the chronological approaches used to interpret these Quaternary records, particularly over timescales that lie beyond the upper age range of radiocarbon (¹⁴C) dating.

The main aim of this thesis is to provide an improved, numerical-age, chronostratigraphic framework for Quaternary environmental

reconstructions in eastern Beringia. For this purpose, optically stimulated luminescence (OSL) and infrared stimulated luminescence (IRSL) dating techniques are used to provide chronological constraints on key stratigraphic units containing correlative tephra horizons within Pleistocene loess and glaciofluvial gravels from eastern Alaska and the Yukon Territory. Importantly, the suitability of OSL dating of tephra-bearing deposits in this region remains to be fully investigated, and this forms an integral part of the research undertaken in this thesis. To do this, single-grain and multi-grain OSL dating techniques were applied to 140,000 to 30,000 year-old deposits associated with geochemically-characterised Late Pleistocene tephra layers from the Yukon Territory (Klondike district, Ash Bend, Ch'ijee's Bluff) and eastern Alaska (Chester Bluff), which have been constrained by independent age control (^{14}C and fission-track ages). Multi-grain feldspar IRSL dating was also conducted on these known-age tephra-bearing deposits using a range of emission bands (ultraviolet, blue, yellow and orange-red emissions). An additional objective of the research was to investigate the OSL behavioural characteristics and grain-to-grain variability of sedimentary quartz grains from this region, as a means of developing more reliable single-grain and multi-grain OSL chronologies.

The single-aliquot regenerative-dose protocol was found to be well suited for dating both quartz and feldspar fractions of these tephra-bearing deposits. Sedimentary quartz grains from this region were, however, generally characterised by dim OSL signals. A key finding of this study was that multi-grain OSL dating of known-age deposits typically resulted in severe age underestimation. Several possible reasons for this were explored through signal-component investigations and the construction of „synthetic“ aliquots from single-grain measurements. Single-grain OSL dating produced widely spread (overdispersed) dose distributions, but ages that are in broad agreement with independent age control when using either of two well-established models to estimate the burial dose (the central and minimum age models). The findings of this thesis indicate that single-grain quartz OSL techniques are better suited to dating loess deposits in this region than are multi-grain quartz OSL techniques, because the former allow for the exclusion of aberrant grains that are particularly prominent in these samples. A major source of uncertainty in the OSL dating of these perennially-frozen deposits was the long-term water content during their burial periods. In some instances, the OSL ages obtained using the „as measured“ water content greatly underestimated the expected ages of the deposits. Investigations into the multi-grain feldspar IRSL characteristics showed that

anomalous fading was ubiquitous in these samples, regardless of the emission band. In most cases, however, it was possible to derive IRSL ages that were in agreement with the corresponding single-grain quartz OSL ages by applying suitable fading-correction procedures.

This thesis represents the first comprehensive study to apply single-grain OSL dating techniques to eastern Beringian deposits and provides some of the first OSL-based numerical-age constraints for both existing tephrochronologies and newly-identified tephra across Alaska and the Yukon Territory. The OSL chronologies established in this study include (i) maximum and minimum age constraints on the Reid glacial deposits (which represent the penultimate advance of the Cordilleran ice sheet) in central Yukon Territory; (ii) a depositional age for numerous, but previously undated, Late Pleistocene tephra in this region; (iii) the first numerical ages for the interglacial deposits and Old Crow tephra at Ch'ijee's Bluff; and (iv) numerical age constraints on extensive Pleistocene loess and organic beds at Chester Bluff.

Author: Jin Cheul Kim
Thesis Title: Geochronology and geochemical characteristics of sediments at the Jeongokri archaeological site, Korea²
Grade: PhD
Date: August, 2009
Supervisors: Yong Il Lee, Geoff Duller, Helen Roberts
Address: Korea Institute of Geoscience and Mineral Resources, 92 Gwahang-no, Yuseong-gu, Daejeon 305-350, KOREA

This study presents the depositional ages and geochemical characteristics of unconsolidated Quaternary sediments collected from the Jeongokri archaeological area, Korea. For decades, many paleolithic artifacts have been excavated from this area, which provided important data for the East Asian Lower Palaeolithic with occurrence of the so-called „Acheulian-like“ handaxe (Yi and Clark, 1983; Bae, 1988). Unconsolidated sediments from a total of 12 localities at the Jeongokri were collected from the sediment sequence overlying unconformably the Quaternary Jeongok Basalt. Among them, 25 samples were selected from three places for age dating. Age

² The full text of this thesis is available online at www.aber.ac.uk/ancient-tl

estimate was made by applying of optically stimulated luminescence (OSL) dating, with results showing a large range of age distribution. The samples collected from fluvial sandy sediments at locality 1 have an age range of 34 to 66 ka, while those from fine-grained silty-clay sediments (localities 2 and 3) are with a range of 100 to 200 ka. Localities 2 and 3 do not show ages younger than 100 ka. The altitude of the Jeongok Basalt beds indicates the possible existence of least three different basalt levels at 48~49 m, 52 m, 53~54 m above the sea-level. Previous age-dating suggested that the lava flow could have occurred during a prolonged period between 0.1 and 0.5 Ma (Kojima, 1983; Danhara et al., 2002; Yi et al., 2005). The current study demonstrates that the deposition of the unconsolidated fine-grained sediments on the basalt bed began at least 200,000 years ago. Re-measurement of the artifact horizon by OSL dating suggests that a hominin occupation could be younger (less than 200 ka) than previously suggested. The results of geochemical analyses suggest that the most dominant sources of the deposit could be the Chinese loess and local material of fluvial origin from the Korean Peninsula. A possible source area of deposition of wind-blown materials is the Yellow Sea locating between China and Korea. Also, geochemical compositions of the deposit indicate the influence of monsoonal activities on the Quaternary paleoenvironment in Korea, which are closely related with sediments origin.

Bibliography

Compiled by Daniel Richter

From 1st May 2009 to 31st October 2009

Allard, T., and Calas, G. (2009). Radiation effects on clay mineral properties. *Applied Clay Science* **43**, 143-149.

Almeida-Filho, R., Rossetti, D. F., Miranda, F. P., Ferreira, F. J., Silva, C., and Beisl, C. (2009). Quaternary reactivation of a basement structure in the Barreirinhas Basin, Brazilian Equatorial Margin. *Quaternary Research* **72**, 103-110.

Antoine, P., Rousseau, D.-D., Moine, O., Kunesch, S., Hatté, C., Lang, A., Tissoux, H., and Zöller, L. (2009). Rapid and cyclic aeolian deposition during the Last Glacial in European loess: a high-resolution record from Nussloch, Germany. *Quaternary Science Reviews* **28**, 2955-2973.

Athanassas, C., and Zacharias, N. (2010). Recuperated-OSL dating of quartz from Aegean (South Greece) raised Pleistocene marine sediments: current results. *Quaternary Geochronology* **5**, 65-75.

Barton, R. N. E., Bouzouggar, A., Collcutt, S. N., Schwenninger, J. L., and Clark-Balzan, L. (2009). OSL dating of the Aterian levels at Dar es-Soltan I (Rabat, Morocco) and implications for the dispersal of modern Homo sapiens. *Quaternary Science Reviews* **28**, 1914-1931.

Bauer, C., Raich, H., Jeschke, G., and Blümmler, P. (2009). Design of a permanent magnet with a mechanical sweep suitable for variable-temperature continuous-wave and pulsed EPR spectroscopy. *Journal of Magnetic Resonance* **198**, 222-227.

Berger, G. W. (2009). Zeroing tests of luminescence sediment dating in the Arctic Ocean: Review and new results from Alaska-margin core tops and central-ocean dirty sea ice. *Global And Planetary Change* **68**, 48-57.

Berger, G. W., Ante, S., and Domack, E. W. (2009). Seasonal and water-depth variations in sediment luminescence and in sedimentation from sediment trap samples at Gerlache Strait, Antarctic Peninsula. *Antarctic Science* **21**, 483-499.

Berger, G. W., Post, S., and Wenker, C. (2009). Single and multigrain quartz-luminescence dating of irrigation-channel features in Santa Fe, New Mexico. *Geoarchaeology* **24**, 383-401.

Boguckij, A. B., Lanczont, M., Lacka, B., Madeyska, T., and Sytnyk, O. (2009). Age and the palaeoenvironment of the West Ukrainian palaeolithic: the case of Velykyi Glybochok multi-cultural site. *Journal of Archaeological Science* **36**, 1376-1389.

Bokhorst, M. P., Beets, C. J., Markovic, S. B., Gerasimenko, N. P., Matviishina, Z. N., and Frechen, M. (2009). Pedo-chemical climate proxies in Late Pleistocene Serbian-Ukrainian loess sequences. *Quaternary International* **198**, 113-123.

Braillard, L., and Guelat, M. (2008). Une nappe alluviale étagée du pléistocène supérieur dans la vallée de Delémont (Jura suisse): lithostratigraphie et datation. *Quaternaire* **19**, 217-228.

Brown, K. S., Marean, C. W., Herries, A. I. R., Jacobs, Z., Tribolo, C., Braun, D., Roberts, D. L., Meyer, M. C., and Bernatchez, J. (2009). Fire As an Engineering Tool of Early Modern Humans. *Science* **325**, 859-862.

Buckman, S., Brownlie, K. C., Bourman, R. P., Murray-Wallace, C. V., Morris, R. H., Lachlan, T. J., Roberts, R. G., Arnold, L. J., and Cann, J. H. (2009). Holocene palaeofire records in a high-level, proximal valley-fill (Wilson Bog), Mount Lofty Ranges, South Australia. *The Holocene* **19**, 1017-1029.

Burrough, S. L., Thomas, D. S. G., and Bailey, R. M. (2009). Mega-Lake in the Kalahari: A Late Pleistocene record of the Palaeolake Makgadikgadi system. *Quaternary Science Reviews* **28**, 1392-1411.

Busschers, F. S., van Balen, R. T., Cohen, K. M., Kasse, C., Weerts, H. J. T., Wallinga, J., and Bunnik, F. P. M. (2008). Response of the Rhine-Meuse fluvial system to Saalian ice-sheet dynamics. *Boreas* **37**, 377-398.

Cano, N. F., Arizaca, E. C., Yauri, J. M., Arenas, J. S. A., and Watanabe, S. (2009). Dating archeological ceramics from the Valley of Vitor, Arequipa by the TL method. *Radiation Effects and Defects in Solids* **164**, 572 - 577.

Chen, R., Pagonis, V., and Lawless, J. L. (2009). A new look at the linear-modulated optically stimulated luminescence (LM-OSL) as a tool for dating and dosimetry. *Radiation Measurements* **44**, 344-350.

Chruscinska, A. (2009). Modelling the thermal bleaching of OSL signal in the case of a competition between recombination centres. *Radiation Measurements* **44**, 329-337.

Cordier, S., Frechen, M., and Harmand, D. (2009). The Pleistocene fluvial deposits of the Moselle and middle Rhine valleys: new correlations and compared evolutions. *Quaternaire* **20**, 35-47.

Costantini, E. A. C., Priori, S., Urban, B., Hilgers, A., Sauer, D., Protano, G., Trombino, L., Hülle, D., and Nannoni, F. (2009). Multidisciplinary characterization of the middle Holocene eolian deposits of the Elsa River basin (central Italy). *Quaternary International* **209**, 107-130.

Darrénougué, N., De Deckker, P., Fitzsimmons, K. E., Norman, M. D., Reed, L., van der Kaars, S., and Fallon, S. (2009). A late Pleistocene record of aeolian sedimentation in Blanche Cave, Naracoorte, South Australia. *Quaternary Science Reviews* **28**, 2600-2615.

Derese, C., Vandenberghe, D., Paulissen, E., and Van den haute, P. (2009). Revisiting a type locality for Late Glacial aeolian sand deposition in NW Europe: Optical dating of the dune complex at Oprimbie (NE Belgium). *Geomorphology* **109**, 27-35.

Despriée, J., Voinchet, P., Gageonnet, R., Dépont, J., Bahain, J.-J., Falguères, C., Tissoux, H., Dolo, J.-M., and Courcimault, G. (2009). Les vagues de peuplements humains au Pléistocène inférieur et moyen dans le bassin de la Loire moyenne, région Centre, France. Apports de l'étude des formations fluviatiles. *L'Anthropologie* **113**, 125-167.

Erginal, A. E., Kiyak, N. G., and Ozcan, H. (2009). Optically stimulated luminescence to date coastal dunes and a possible tsunami layer on the Kavak Delta (Saras Gulf, NW Turkey). *Turkish Journal of Earth Sciences* **18**, 465-474.

Farias, T. M. B., Gennari, R. F., Chubaci, J. F. D., and Watanabe, S. (2009). FTIR spectra and TL properties of quartz annealed at high temperatures. *Physics Procedia* **2**, 493-496.

Farias, T. M. B., Gennari, R. F., Etchevarne, C., and Watanabe, S. (2009). Thermoluminescence dating of Brazilian indigenous ceramics. *Radiat Prot Dosimetry* **136**, 45-49.

Farias, T. M. B., Watanabe, S., and Gundu Rao, T. K. (2009). Defect centre responsible for production of 110° C TL peak in quartz. *Solid State Communications* **149**, 1173-1175.

Fitzsimmons, K. E., Magee, J. W., and Amos, K. J. (2009). Characterisation of aeolian sediments from the Strzelecki and Tirari Deserts, Australia: Implications for reconstructing palaeoenvironmental conditions. *Sedimentary Geology* **218**, 61-73.

- Fitzsimmons, K. E., and Telfer, M. W. (2008). Sedimentary history and the interpretation of late Quaternary dune records: Examples from the Tirari desert, Australia and the Kalahari, South Africa. *Chungara-Revista De Antropologia Chilena* **40**, 295-308.
- Fornós, J. J., Clemmensen, L. B., Gómez-Pujol, L., and Murray, A. S. (2009). Late Pleistocene carbonate aeolianites on Mallorca, Western Mediterranean: a luminescence chronology. *Quaternary Science Reviews* **28**, 2697-2709.
- Frechen, M., Seifert, B., Sanabria, J. A., and Argüello, G. L. (2009). Chronology of late Pleistocene Pampa loess from the Córdoba area in Argentina. *Journal of Quaternary Science* **24**, 761-772.
- Fuchs, M., and Lang, A. (2009). Luminescence dating of hillslope deposits-A review. *Geomorphology* **109**, 17-26.
- Garcia, A. F., and Mahan, S. A. (2009). Sediment storage and transport in Pancho Rico Valley during and after the Pleistocene-Holocene transition, Coast Ranges of central California (Monterey County). *Earth Surface Processes and Landforms* **34**, 1136-1150.
- Gartia, R. K. (2009). Paleothermometry of NaCl as evidenced from thermoluminescence data. *Nuclear Instruments and Methods in Physics Research Section B: Beam Interactions with Materials and Atoms* **267**, 2903-2907.
- Gemmell, A. M. D., and Spötl, C. (2009). Attempts to date the Hötting Breccia near Innsbruck (Austria), a classical Quaternary site in the Alps, by optically-stimulated luminescence. *Austrian Journal of Earth Sciences* **102**, 50-61.
- Greilich, S., and Wagner, G. A. (2009). Light Thrown on History – The Dating of Stone Surfaces at the Geoglyphs of Palpa Using Optically Stimulated Luminescence. In "New Technologies for Archaeology." (M. Reindel, and G. A. Wagner, Eds.), pp. 271-283. Springer, Berlin.
- Habertzell, T., Anselmetti, F. S., Bowen, S. W., Fey, M., Mayr, C., Zolitschka, B., Ariztegui, D., Mauz, B., Ohlendorf, C., Kastner, S., Lücke, A., Schäbitz, F., and Wille, M. (2009). Late Pleistocene dust deposition in the Patagonian steppe - extending and refining the paleoenvironmental and tephrochronological record from Laguna Potrok Aike back to 55 ka. *Quaternary Science Reviews* **28**, 2927-2939.
- Hülle, D., Hilgers, A., Kühn, P., and Radtke, U. (2009). The potential of optically stimulated luminescence for dating periglacial slope deposits -- A case study from the Taunus area, Germany. *Geomorphology* **109**, 66-78.
- Jaek, I., Molodkov, A., and Vasilchenko, V. (2008). Instability of luminescence responses in feldspar-and quartz-based paleo-dosimeters. *Journal of Applied Spectroscopy* **75**, 820-825.
- Jensen, M. A., Demidov, I. N., Larsen, E., and Lyså, A. (2009). Quaternary palaeoenvironments and multi-storey valley fill architecture along the Mezen and Severnaya Dvina river valleys, Arkhangelsk region, NW Russia. *Quaternary Science Reviews* **28**, 2489-2506.
- Jiang, H. C., Wang, P., Thompson, J., Ding, Z. L., and Lu, Y. C. (2009). Last glacial climate instability documented by coarse-grained sediments within the loess sequence, at Fanjiaping, Lanzhou, China. *Quaternary Research* **72**, 91-102.
- Kadereit, A., Greilich, S., Woda, C., and Wagner, G. A. (2009). Cold Light from the Sediments of a Hot Desert: How Luminescence Dating Sheds Light on the Landscape Development of the Northeastern Atacama. In "New Technologies for Archaeology." (M. Reindel, and G. A. Wagner, Eds.), pp. 245-270. Springer, Berlin.
- Kaiser, K., Hilgers, A., Schlaak, N., Jankowski, M., Kühn, P., Bussemer, S., and Przegietka, K. (2009). Palaeopedological marker horizons in northern central Europe: characteristics of Lateglacial Usselo and Finow soils. *Boreas* **38**, 591-609.

- Kaiser, K., Lai, Z. P., Schneider, B., Schoch, W. H., Shen, X. H., Miede, G., and Brückner, H. (2009). Sediment sequences and paleosols in the Kyichu Valley, southern Tibet (China), indicating Late Quaternary environmental changes. *Island Arc* **18**, 404-427.
- Kitis, G., Kiyak, N., Polymeris, G. S., and Tsirliganis, N. C. (2010). The correlation of fast OSL component with the TL peak at in quartz of various origins. *Journal of Luminescence* **130**, 298-303.
- Kock, S., Huggenberger, P., Preusser, F., Rentzel, P., and Wetzel, A. (2009). Formation and evolution of the Lower Terrace of the Rhine River in the area of Basel. *Swiss Journal of Geosciences* **102**, 307-321.
- Kock, S., Kramers, J. D., Preusser, F., and Wetzel, A. (2009). Dating of Late Pleistocene terrace deposits of the River Rhine using Uranium series and luminescence methods: Potential and limitations. *Quaternary Geochronology* **4**, 363-373.
- Lai, Z., Kaiser, K., and Brückner, H. (2009). Luminescence-dated aeolian deposits of late Quaternary age in the southern Tibetan Plateau and their implications for landscape history. *Quaternary Research* **72**, 421-430.
- Lair, G. J., Zehetner, F., Hrachowitz, M., Franz, N., Maringer, F.-J., and Gerzabek, M. H. (2009). Dating of soil layers in a young floodplain using iron oxide crystallinity. *Quaternary Geochronology* **4**, 260-266.
- Le Dortz, K., Meyer, B., Sebrier, M., Nazari, H., Braucher, R., Fattahi, M., Benedetti, L., Foroutan, M., Siame, L., Bourles, D., Talebian, M., Bateman, M. D., and Ghorraishi, M. (2009). Holocene right-slip rate determined by cosmogenic and OSL dating on the Anar fault, Central Iran. *Geophysical Journal International* **179**, 700-710.
- Lepper, K. (2009). The effect of evaporated salt solutions on the optical dating properties of JSC Mars-1: "seasoning" for a Mars soil simulant. *Astrobiology* **9**, 531-534.
- Liu, H., Kishimoto, S., Takagawa, T., Shirai, M., and Sato, S. (2009). Investigation of the sediment movement along the Tenryu-Enshunada fluvial system based on feldspar thermoluminescence properties. *Journal of Coastal Research* **25**, 1096-1105.
- Madsen, A. T., Duller, G. A. T., Donnelly, J. P., Roberts, H. M., and Wintle, A. G. (2009). A chronology of hurricane landfalls at Little Sippewissett Marsh, Massachusetts, USA, using optical dating. *Geomorphology* **109**, 36-45.
- Madsen, A. T., and Murray, A. S. (2009). Optically stimulated luminescence dating of young sediments: A review. *Geomorphology* **109**, 3-16.
- Marchal, F., Monchot, H., Coussot, C., Desclaux, E., Deschamp, P., Thiébaud, C., Bahain, J.-J., Falguères, C., and Dolo, J.-M. (2009). Neandertals paleoenvironment in Western Provence: The contribution of Les Auzières 2 (Méthamis, Vaucluse, France). *Comptes Rendus Palevol* **8**, 493-502.
- Markovic, S. B., Hambach, U., Catto, N., Jovanovic, M., Buggle, B., Machalet, B., Zöller, L., Glaser, B., and Frechen, M. (2009). Middle and Late Pleistocene loess sequences at Batajnica, Vojvodina, Serbia. *Quaternary International* **198**, 255-266.
- Mason, J. A., Lu, H., Zhou, Y., Miao, X., Swinehart, J. B., Liu, Z., Goble, R. J., and Yi, S. (2009). Dune mobility and aridity at the desert margin of northern China at a time of peak monsoon strength. *Geology* **37**, 947-950.
- Mauz, B., Elmejdoub, N., Nathan, R., and Jedoui, Y. (2009). Last interglacial coastal environments in the Mediterranean-Saharan transition zone. *Palaeogeography, Palaeoclimatology, Palaeoecology* **279**, 137-146.

- Mebhah, D., Imatoukene, D., Lounis-Mokrani, Z., and Kechouane, M. (2009). Comparative study on the effect of annealing treatments on RTL mechanism in natural quartz from different origins. *Journal of Luminescence* **129**, 1615-1618.
- Mercader, J., Asmerom, Y., Bennett, T., Raja, M., and Skinner, A. (2009). Initial excavation and dating of Ngalue Cave: A Middle Stone Age site along the Niassa Rift, Mozambique. *Journal of Human Evolution* **57**, 63-74.
- Molodkov, A., and Bolikhovskaya, N. (2009). Climate change dynamics in Northern Eurasia over the last 200 ka: Evidence from mollusc-based ESR-chronostratigraphy and vegetation successions of the loess-palaeosol records. *Quaternary International* **201**, 67-76.
- Murray-Wallace, C. V., Bourman, R. P., Prescott, J. R., Williams, F., Price, D. M., and Belperio, A. P. (2010). Aminostratigraphy and thermoluminescence dating of coastal aeolianites and the later Quaternary history of a failed delta: The River Murray mouth region, South Australia. *Quaternary Geochronology* **5**, 28-49.
- Nissen, E., Walker, R. T., Bayasgalan, A., Carter, A., Fattahi, M., Molor, E., Schnabel, C., West, A. J., and Xu, S. (2009). The late Quaternary slip-rate of the Har-Us-Nuur fault (Mongolian Altai) from cosmogenic ¹⁰Be and luminescence dating. *Earth And Planetary Science Letters* **286**, 467-478.
- Nott, J., Smithers, S., Walsh, K., and Rhodes, E. (2009). Sand beach ridges record 6000 year history of extreme tropical cyclone activity in northeastern Australia. *Quaternary Science Reviews* **28**, 1511-1520.
- Owen, L. A., Robinson, R., Benn, D. I., Finkel, R. C., Davis, N. K., Yi, C., Putkonen, J., Li, D., and Murray, A. S. (2009). Quaternary glaciation of Mount Everest. *Quaternary Science Reviews* **28**, 1412-1433.
- Pagonis, V., Ankjærsgaard, C., Murray, A. S., and Chen, R. (2009). Optically stimulated exoelectron emission processes in quartz: comparison of experiment and theory. *Journal of Luminescence* **129**, 1003-1009.
- Pan, Y. M., and Hu, B. Q. (2009). Radiation-induced defects in quartz. IV. Thermal properties and implications. *Physics and Chemistry of Minerals* **36**, 421-430.
- Pietsch, T. J. (2009). Optically stimulated luminescence dating of young (<500 years old) sediments: Testing estimates of burial dose. *Quaternary Geochronology* **4**, 406-422.
- Polat, M., and Korkmaz, M. (2009). The effects of temperature on ESR spectrum of gamma-irradiated ammonium tartrate. *Radiation Physics and Chemistry* **78**, 966-970.
- Porat, N., Chazan, M., Grün, R., Aubert, M., Eisenmann, V., and Horwitz, L. K. (2010). New radiometric ages for the Fauresmith industry from Kathu Pan, southern Africa: Implications for the Earlier to Middle Stone Age transition. *Journal of Archaeological Science* **37**, 269-283.
- Ramasamy, V., Ponnusamy, V., Gomathi, S. S., and Jose, M. T. (2009). Thermostimulated luminescence characteristics of dolomitic rocks and their use as a gamma ray dosimeter. *Radiation Measurements* **44**, 351-358.
- Ramsthaler, F., Kreutz, K., Zipp, K., and Verhoff, M. A. (2009). Dating skeletal remains with luminol-chemiluminescence. Validity, intra- and interobserver error. *Forensic Science International* **187**, 47-50.
- Ranjbar, A. H., Aliabadi, R., Amraei, R., Tabasi, M., and Mirjalily, G. (2009). ESR response of bulk samples of clear fused quartz (CFQ) material to high doses from 10 MeV electrons: Its possible application for radiation processing and medical sterilization. *Applied Radiation and Isotopes* **67**, 1023-1026.
- Rey, L., Gartia, R. K., Bishal Singh, K., and Basanta Singh, T. (2009). Thermoluminescence of ice and its implications. *Nuclear Instruments and Methods in Physics Research Section B: Beam Interactions with Materials and Atoms* **267**, 3633-3639.

- Roberts, R. G., Westaway, K. E., Zhao, J. x., Turney, C. S. M., Bird, M. I., Rink, W. J., and Fifield, L. K. (2009). Geochronology of cave deposits at Liang Bua and of adjacent river terraces in the Wae Racang valley, western Flores, Indonesia: a synthesis of age estimates for the type locality of *Homo floresiensis*. *Journal of Human Evolution* **57**, 484-502.
- Roberts, S. J., Hodgson, D. A., Bentley, M. J., Sanderson, D. C. W., Milne, G., Smith, J. A., Verleyen, E., and Balbo, A. (2009). Holocene relative sea-level change and deglaciation on Alexander Island, Antarctic Peninsula, from elevated lake deltas. *Geomorphology* **112**, 122-134.
- Rudko, V. V., Vorona, I. P., Baran, N. R., and Ishchenko, S. S. (2009). Thermally stimulated transformation of the EPR spectra in gamma-irradiated bone tissue. *Radiation Measurements* **44**, 239-242.
- Santoro, E., Mazzella, M. E., Ferranti, L., Randisi, A., Napolitano, E., Rittner, S., and Radtke, U. (2009). Raised coastal terraces along the Ionian Sea coast of northern Calabria, Italy, suggest space and time variability of tectonic uplift rates. *Quaternary International* **206**, 78-101.
- Schultze, C. A., Stanish, C., Scott, D. A., Rehren, T., Kuehner, S., and Feathers, J. K. (2009). Direct evidence of 1,900 years of indigenous silver production in the Lake Titicaca Basin of Southern Peru. *Proceedings of the National Academy of Sciences* **106**, 17280-17283.
- Schwanghart, W., Frechen, M., Kuhn, N. J., and Schütt, B. (2009). Holocene environmental changes in the Uggii Nuur basin, Mongolia. *Palaeogeography, Palaeoclimatology, Palaeoecology* **279**, 160-171.
- Sinha, R., Kettanah, Y., Gibling, M. R., Tandon, S. K., Jain, M., Bhattacharjee, P. S., Dasgupta, A. S., and Ghazanfari, P. (2009). Craton-derived alluvium as a major sediment source in the Himalayan Foreland Basin of India. *Geological Society of America Bulletin* **121**, 1596-1610.
- Stefanaki, E. C., Afouxenidis, D., Polymeris, G. S., Sakalis, A., Tsirliganis, N. C., and Kitis, G. (2009). Optically Stimulated Luminescence properties of natural Schist. *Mediterranean Archaeology & Archaeometry* **9**, 1-16.
- Steffen, D., Preusser, F., and Schlunegger, F. (2009). OSL quartz age underestimation due to unstable signal components. *Quaternary Geochronology* **4**, 353-362.
- Steffen, D., Schlunegger, F., and Preusser, F. (2009). Drainage basin response to climate change in the Pisco valley, Peru. *Geology* **37**, 491-494.
- Thomas, P. J. (2009). Luminescence dating of beachrock in the southeast coast of India - potential for Holocene shoreline reconstruction. *Journal of Coastal Research* **25**, 1-7.
- Thrasher, I. M., Mauz, B., Chiverrell, R. C., Lang, A., and Thomas, G. S. P. (2009). Testing an approach to OSL dating of Late Devensian glaciofluvial sediments of the British Isles. *Journal of Quaternary Science* **24**, 785-801.
- Titschack, J., Radtke, U., and Freiwald, A. (2009). Dating and characterization of polymorphic transformation of aragonite to calcite in Pleistocene bivalves from Rhodes (Greece) by combined shell microstructure, stable isotope, and Electron Spin Resonance study. *Journal of Sedimentary Research* **79**, 332-346.
- Vermeesch, P. (2009). RadialPlotter: A Java application for fission track, luminescence and other radial plots. *Radiation Measurements* **44**, 409-410.
- von Suchodoletz, H., Kühn, P., Hambach, U., Dietze, M., Zöller, L., and Faust, D. (2009). Loess-like and palaeosol sediments from Lanzarote (Canary Islands/Spain) - Indicators of palaeoenvironmental change during the Late Quaternary. *Palaeogeography, Palaeoclimatology, Palaeoecology* **278**, 71-87.

- Wang, W. D. (2009). Study and progress of the thermoluminescence dating of the ancient pottery and porcelain. *Science in China Series E-Technological Sciences* **52**, 1613-1640.
- Wolfe, S. A., and Hugenholtz, C. H. (2009). Barchan dunes stabilized under recent climate warming on the northern Great Plains. *Geology* **37**, 1039-1042.
- Wolfe, S. A., Walker, I. J., and Huntley, D. J. (2008). Holocene coastal reconstruction, Naikoon peninsula, Queen Charlotte Islands, British Columbia. Current Research, Geological Survey of Canada, Report-No: 2008-12
- Wysota, W., Molewski, P., and Sokolowski, R. J. (2009). Record of the Vistula ice lobe advances in the Late Weichselian glacial sequence in north-central Poland. *Quaternary International* **207**, 26-41.
- Xu, L., and Zhou, S. (2009). Quaternary glaciations recorded by glacial and fluvial landforms in the Shaluli Mountains, Southeastern Tibetan Plateau. *Geomorphology* **103**, 268-275.
- Xu, X., Yang, J., Dong, G., Wang, L., and Miller, L. (2009). OSL dating of glacier extent during the Last Glacial and the Kanas Lake basin formation in Kanas River valley, Altai Mountains, China. *Geomorphology* **112**, 306-317.
- Yuan, Q. D., Zhang, Z. C., Wu, C. D., and Guo, Z. J. (2009). Age and Provenance of Loess deposits on the Northern Flank of Tianshan Mountain. *Acta Geologica Sinica-English Edition* **83**, 648-654.
- Zacharias, N., Bassiakos, Y., Hayden, B., Theodorakopoulou, K., and Michael, C. T. (2009). Luminescence dating of deltaic deposits from eastern Crete, Greece: Geoarchaeological implications. *Geomorphology* **109**, 46-53.
- Zembo, I., Panzeri, L., Galli, A., Bersezio, R., Martini, M., and Sibilìa, E. (2009). Quaternary evolution of the intermontane Val d'Agri Basin, Southern Apennines. *Quaternary Research* **72**, 431-442.
- Zhang, J.-F., Qiu, W.-L., Li, R.-Q., and Zhou, L.-P. (2009). The evolution of a terrace sequence along the Yellow River (HuangHe) in Hequ, Shanxi, China, as inferred from optical dating. *Geomorphology* **109**, 54-65.

Papers from the Beijing LED08 conference published in Volume 44/5-6 of Radiation Measurements

- Ankjærgaard, C., Jain, M., Kalchgruber, R., Lapp, T., Klein, D., McKeever, S. W. S., Murray, A. S., and Morthekai, P. (2009). Further investigations into pulsed optically stimulated luminescence from feldspars using blue and green light. *Radiation Measurements* **44**, 576-581.
- Beerten, K., Woda, C., and Vanhavere, F. (2009). Thermoluminescence dosimetry of electronic components from personal objects. *Radiation Measurements* **44**, 620-625.
- Biswas, R. H., Murari, M. K., and Singhvi, A. K. (2009). Dose-dependent change in the optically stimulated luminescence decay of Al₂O₃:C. *Radiation Measurements* **44**, 543-547.
- Bos, A. J. J., and Wallinga, J. (2009). Analysis of the quartz OSL decay curve by differentiation. *Radiation Measurements* **44**, 588-593.
- Burbidge, C. I., Dias, M. I., Prudêncio, M. I., Rebêlo, L. P., Cardoso, G., and Brito, P. (2009). Internal α activity: localisation, compositional associations and effects on OSL signals in quartz approaching β saturation. *Radiation Measurements* **44**, 494-500.

Buylaert, J. P., Murray, A. S., Thomsen, K. J., and Jain, M. (2009). Testing the potential of an elevated temperature IRSL signal from K-feldspar. *Radiation Measurements* **44**, 560-565.

Chauhan, N., Anand, S., Palani Selvam, T., Mayya, Y. S., and Singhvi, A. K. (2009). Extending the maximum age achievable in the luminescence dating of sediments using large quartz grains: A feasibility study. *Radiation Measurements* **44**, 629-633.

Chen, S., Liu, X., Zhang, C., and Tang, Q. (2009). The Monte Carlo simulation of the absorbed dose in quartz. *Radiation Measurements* **44**, 626-628.

Chithambo, M. L., and Ogundare, F. O. (2009). Luminescence lifetime components in quartz: Influence of irradiation and annealing. *Radiation Measurements* **44**, 453-457.

Choi, J. H., Murray, A. S., Cheong, C. S., and Hong, S. C. (2009). The dependence of dose recovery experiments on the bleaching of natural quartz OSL using different light sources. *Radiation Measurements* **44**, 600-605.

Cunningham, A. C., and Wallinga, J. (2009). Optically stimulated luminescence dating of young quartz using the fast component. *Radiation Measurements* **44**, 423-428.

Duller, G. A. T., Penkman, K. E. H., and Wintle, A. G. (2009). Assessing the potential for using biogenic calcites as dosimeters for luminescence dating. *Radiation Measurements* **44**, 429-433.

Duval, M., Grün, R., Falguères, C., Bahain, J. J., and Dolo, J. M. (2009). ESR dating of Lower Pleistocene fossil teeth: Limits of the single saturating exponential (SSE) function for the equivalent dose determination. *Radiation Measurements* **44**, 477-482.

Fan, A., Li, S.-H., and Li, B. (2009). Characteristics of quartz infrared stimulated luminescence (IRSL) at elevated temperatures. *Radiation Measurements* **44**, 434-438.

Ganzawa, Y., and Maeda, M. (2009). 390-410 °C isothermal red thermoluminescence (IRTL) dating of volcanic quartz using the SAR method. *Radiation Measurements* **44**, 517-522.

Gao, L., Yin, G.-M., Liu, C.-R., Bahain, J.-J., Lin, M., and Li, J.-P. (2009). Natural sunlight bleaching of the ESR titanium center in quartz. *Radiation Measurements* **44**, 501-504.

Grün, R. (2009). The relevance of parametric U-uptake models in ESR age calculations. *Radiation Measurements* **44**, 472-476.

Guibert, P., Bailiff, I. K., Blain, S., Gueli, A. M., Martini, M., Sibilia, E., Stella, G., and Troja, S. O. (2009). Luminescence dating of architectural ceramics from an early medieval abbey: The St Philbert Intercomparison (Loire Atlantique, France). *Radiation Measurements* **44**, 488-493.

Jain, M. (2009). Extending the dose range: Probing deep traps in quartz with 3.06 eV photons. *Radiation Measurements* **44**, 445-452.

Jaiswal, M. K., Bhat, M. I., Bali, B. S., Ahmad, S., and Chen, Y. G. (2009). Luminescence characteristics of quartz and feldspar from tectonically uplifted terraces in Kashmir Basin, Jammu and Kashmir, India. *Radiation Measurements* **44**, 523-528.

Joannes-Boyau, R., and Grün, R. (2009). Thermal behavior of orientated and non-orientated CO₂- radicals in tooth enamel. *Radiation Measurements* **44**, 505-511.

- Kars, R. H., and Wallinga, J. (2009). IRSL dating of K-feldspars: Modelling natural dose response curves to deal with anomalous fading and trap competition. *Radiation Measurements* **44**, 594-599.
- Lapp, T., Jain, M., Ankjærgaard, C., and Pirtzel, L. (2009). Development of pulsed stimulation and Photon Timer attachments to the Risø TL/OSL reader. *Radiation Measurements* **44**, 571-575.
- Larsen, A., Greilich, S., Jain, M., and Murray, A. S. (2009). Developing a numerical simulation for fading in feldspar. *Radiation Measurements* **44**, 467-471.
- Lawless, J. L., Chen, R., and Pagonis, V. (2009). Sublinear dose dependence of thermoluminescence and optically stimulated luminescence prior to the approach to saturation level. *Radiation Measurements* **44**, 606-610.
- Martini, M., Fasoli, M., and Galli, A. (2009). Quartz OSL emission spectra and the role of [AlO₄]^o recombination centres. *Radiation Measurements* **44**, 458-461.
- Murray, A. S., Buylaert, J. P., Thomsen, K. J., and Jain, M. (2009). The effect of preheating on the IRSL signal from feldspar. *Radiation Measurements* **44**, 554-559.
- Nian, X. M., Zhou, L. P., and Qin, J. T. (2009). Comparisons of equivalent dose values obtained with different protocols using a lacustrine sediment sample from Xuchang, China. *Radiation Measurements* **44**, 512-516.
- Pagonis, V., Wintle, A. G., Chen, R., and Wang, X. L. (2009). Simulations of thermally transferred OSL experiments and of the ReSAR dating protocol for quartz. *Radiation Measurements* **44**, 634-638.
- Porat, N., Duller, G. A. T., Roberts, H. M., and Wintle, A. G. (2009). A simplified SAR protocol for TT-OSL. *Radiation Measurements* **44**, 538-542.
- Qin, J. T., and Zhou, L. P. (2009). Stepped-irradiation SAR: A viable approach to circumvent OSL equivalent dose underestimation in last glacial loess of northwestern China. *Radiation Measurements* **44**, 417-422.
- Roberts, H. M., Durcan, J. A., and Duller, G. A. T. (2009). Exploring procedures for the rapid assessment of optically stimulated luminescence range-finder ages. *Radiation Measurements* **44**, 582-587.
- Selo, M., Valladas, H., Mercier, N., Joron, J. L., Bassinot, F., Person, A., and Nouet, J. (2009). Investigations of uranium distribution in flints. *Radiation Measurements* **44**, 615-619.
- Shen, Z., and Mauz, B. (2009). D_e determination of quartz samples showing falling D_e(t) plots. *Radiation Measurements* **44**, 566-570.
- Song, K.-W., Yun, K.-K., and Hong, D.-G. (2009). Radiation response of thermoluminescence glow peaks separated using a glow curve fitting method for red emission from quartz. *Radiation Measurements* **44**, 611-614.
- Stevens, T., Buylaert, J. P., and Murray, A. S. (2009). Towards development of a broadly-applicable SAR TT-OSL dating protocol for quartz. *Radiation Measurements* **44**, 639-645.
- Tan, K., Liu, Z., Zeng, S., Liu, Y., Xie, Y., and Rieser, U. (2009). Three-dimensional thermoluminescence spectra of different origin quartz from Altay Orogenic belt, Xinjiang, China. *Radiation Measurements* **44**, 529-533.
- Toyoda, S., Miura, H., and Tissoux, H. (2009). Signal regeneration in ESR dating of tephra with quartz. *Radiation Measurements* **44**, 483-487.
- Vandenbergh, D. A. G., Jain, M., and Murray, A. S. (2009). Equivalent dose determination using a quartz isothermal TL signal. *Radiation Measurements* **44**, 439-444.

Westaway, K. E. (2009). The red, white and blue of quartz luminescence: A comparison of D_e values derived for sediments from Australia and Indonesia using thermoluminescence and optically stimulated luminescence emissions. *Radiation Measurements* **44**, 462-466.

Woda, C., and Spöttl, T. (2009). On the use of OSL of wire-bond chip card modules for retrospective and accident dosimetry. *Radiation Measurements* **44**, 548-553.

Zheng, C. X., Zhou, L. P., and Qin, J. T. (2009). Difference in luminescence sensitivity of coarse-grained quartz from deserts of northern China. *Radiation Measurements* **44**, 534-537.

Conference Announcements



7th New World Luminescence Dating Workshop 2010

23rd-24th September 2010

The Lux laboratory is pleased to announce that the 7th New World Luminescence Dating Workshop (NWLDW) will be held in Montréal (Québec). Workshop presentations are planned for September 23rd and September 24th, 2010 (Thursday and Friday) at the Université du Québec à Montréal (UQAM). A geological, archaeological and cultural field trip is planned for Saturday the 25th. The weather in Québec at the end of September can be very pleasant, and the field trip will be run into beautifully coloured fall boreal forest. Not to be missed!

Information regarding the workshop will be online on <http://lux.uqam.ca/> as soon as possible.

The first circular will be sent by e-mail to those who contact us following this announcement.

For further information send an e-mail to:

barre.magali@uqam.ca or

huot.sebastien@courrier.uqam.ca

Magali Barré
Sébastien Huot
Michel Lamothe

Département des Sciences de la Terre et de
l'Atmosphère Université du Québec à Montréal

Erratum: LED laboratory lighting

G.W. Berger and C. Kratt

Desert Research Institute, 2215 Raggio Parkway, Reno, NV 89512, USA.
(glenn.berger@dri.edu)

(Received 16 November 2009)

In the 2008 issue of Ancient TL, the article by Berger and Kratt (Volume 26(1), pg. 9) should have said that LEDtronics LED lamps have a rated operating life of $>10^5$ hours, not “>105” hours as printed. There was an error in “typesetting” of the accepted, correct version.